To the Graduate Council:

I am submitting herewith a thesis written by Ronald G. Lutz entitled "Effect of Stilling Chamber Velocity Distortions on the Test Section Flow Angularity in a Transonic Wind Tunnel." I recommend that it be accepted in partial fulfillment of the requirements for the degree of Master of Science, with a major in Mechanical Engineering.

Frank G. Collins

Frank G. Collins, Major Professor

We have read this thesis
and recommend its acceptance:

K C Reddy

Ching-fang Lee

Accepted for the Council:

L Evans Roth

Vice Chancellor
Graduate Studies and Research

P

Thesis
T
.L86
cop.2

# EFFECT OF STILLING CHAMBER VELOCITY DISTORTIONS ON THE TEST SECTION FLOW ANGULARITY IN A TRANSONIC WIND TUNNEL

A Thesis

Presented for the

Master of Science

Degree

The University of Tennessee, Knoxville

Ronald G. Lutz

March 1978

1356439

ACKNOWLEDGEMENTS

The author is very appreciative to the officials of ARO, Inc. for permission to use the results presented herein. Also, thanks are due to the author's supervisor, Mr. W. E. Summers, for his guidance and encouragement in the work. Special thanks are given to Mrs. Mary Young for preparation of the figures and to Mrs. Lena Blocker for typing the manuscript.

Particular appreciation is expressed to the author's academic advisor, Dr. F. G. Collins, for his guidance and encouragement in the planning and preparation of the thesis. The author is also thankful for the efforts of his committee members, Dr. C. F. Lo and Dr. K. C. Reddy.

The research reported herein was sponsored by Headquarters, Arnold Engineering Development Center, Arnold Air Force Station, Tennessee, under Contract F40600-75-C-0001 with ARO, Inc. Reproduction to satisfy the needs of the U. S. Government is authorized.

ABSTRACT

The accuracy of the wind tunnel simulation has been enhanced over the past several years by improvements in instrumentation systems. With a need for testing at wider ranges of model attitudes, however, there has been increased emphasis on improvements to the tunnel flow quality. An experimental investigation was conducted to assess the nature of test section disturbances resulting from velocity distortions in the stilling chamber of a transonic wind tunnel. Steady-state flow angularities were found to exist in the test section flow when velocity disturbances were introduced in the stilling chamber even though a honeycomb section was installed at the inlet of the contraction fairing. The nature of the flow angularities was found to be consistent with the orientation of the velocity disturbance.

Theoretical considerations revealed that the vorticity generated in the stilling chamber by the velocity disturbance was reoriented by the contraction fairing to produce the test section flow angularity.

TABLE OF CONTENTS


| CHAPTER | | PAGE |
|---|---|---|
| I. | INTRODUCTION | 1 |
| | Preliminary Information | 1 |
| | Statement of the Problem | 2 |
| | Organization of the Manuscript | 3 |
| II. | APPARATUS | 4 |
| | Wind Tunnel | 4 |
| | Test Installation | 4 |
| | Instrumentation | 6 |
| III. | TEST DESCRIPTION | 8 |
| | Procedure | 8 |
| | Data Reduction | 8 |
| | Data Uncertainties | 10 |
| IV. | EXPERIMENTAL RESULTS | 12 |
| | Stilling Chamber Velocity Profiles | 12 |
| | Test Section Mach Number Profiles | 14 |
| | Test Section Flow Angularity Distributions | 14 |
| V. | THEORETICAL CONSIDERATIONS | 20 |
| | Vorticity Distribution | 20 |
| | Contraction and Nozzle Flow Model | 21 |
| | Comparative Results | 23 |
| VI. | SUMMARY AND CONCLUSIONS | 26 |
| BIBLIOGRAPHY | | 29 |
| APPENDIX | | 31 |
| VITA | | 72 |

LIST OF FIGURES


| FIGURE | | PAGE |
|---|---|---|
| 1. | Schematic of Tunnel 1T and Associated Equipment | 32 |
| 2. | Schematic of Test Installation | 33 |
| 3. | Photograph of Flow Angle Probe Installation | 34 |
| 4. | Details of Flow Angle Probe | 35 |
| 5. | Tunnel Stilling Chamber and Test Section Nomenclature | 36 |
| 6. | Stilling Chamber Velocity Profile, Open Stilling Chamber | 37 |
| 7. | Stilling Chamber Velocity Profile, Screen Configuration 1 | 39 |
| 8. | Stilling Chamber Velocity Profile, Screen Configuration 5 | 43 |
| 9. | Test Section Mach Number Surveys with and without Screen Configurations 1 and 2 | 48 |
| 10. | The Variation of Test Section Flow Angularity with Vertical Position (z) at Various Lateral (y) Positions for the Open Stilling Chamber Configuration at $M_\infty = 0.6$ | 49 |
| 11. | The Variation of Test Section Flow Angularity with Vertical Position (z) at Various Lateral (y) Positions for the Open Stilling Chamber with the Cruciform Brace Installed | 56 |
| 12. | Resultant Flow Angle Diagram for Screen Configuration 1 | 60 |

FIGURE PAGE

13. Resultant Flow Angle Diagram for Screen Configuration 2 . . . . . 61

14. Resultant Flow Angle Diagram for Screen Configuration 3 . . . . . 62

15. Resultant Flow Angle Diagram for Screen Configuration 4 . . . . . 63

16. Resultant Flow Angle Diagram for Screen Configuration 5 . . . . . 64

17. Resultant Flow Angle Diagram for Screen Configuration 6 . . . . . 65

18. Resultant Flow Angle Diagram for Screen Configuration 7 . . . . . 66

19. Distortion of Lines of Vorticity Encountering a Tree Trunk . . . . . 67

20. Streamline Pattern and Fluid Particle Displacements through a Wind Tunnel Contraction and Nozzle . . . . . 68

21. Illustration of the Reorientation of a Line of Vorticity as it Passes Through the Contraction and Nozzle Resulting in Test Section Flow Angularity . . . . . 69

22. Data Obtained with the Half-Plane Screen in the Right Half of the Stilling Chamber . . . . . 70

## NOMENCLATURE

| | |
|---|---|
| L | Lateral location of rake pressure along rake length, in. |
| $\ell$ | Length of contraction and nozzle, in. |
| $M_\infty$ | Free-stream Mach number |
| MP | Flow angle probe Mach number |
| $p_t$ | Total pressure, psf |
| $p_\infty$ | Free-stream static pressure, psf |
| $q_\infty$ | Free-stream dynamic pressure, psf |
| r | Radius of stilling chamber inlet, in. |
| $T_t$ | Total temperature, °F |
| u | Local velocity in the axial direction, ft/sec |
| V | Local stilling chamber velocity, ft/sec |
| $V_a$ | Average stilling chamber velocity based upon stilling chamber total and static pressures, ft/sec |
| $V_{C.L.}$ | Lateral crossflow velocity on the test section centerline, ft/sec |
| $V/V_a$ | Nondimensional stilling chamber velocity |
| X | Axial location in tunnel with respect to the stilling chamber inlet plane, downstream positive, in. |
| Y | Lateral location in tunnel test section with respect to the tunnel centerline, to the right looking upstream positive, in. |

| | |
|---|---|
| $Z$ | Vertical location in tunnel test section with respect to the tunnel centerline, up positive, in. |
| $\alpha$ | Wind tunnel flow angle in pitch plane, up positive, deg |
| $\rho$ | Free-stream density, $lb/ft^3$ |
| $\phi_P$ | Roll angle of test section survey mechanism, zero with probe near top of tunnel, offset arm vertical, positive clockwise, looking upstream, deg |
| $\phi_R$ | Roll angle of stilling chamber pitot rake, zero with negative pressure locations (-L) below centerline, rake vertical, positive counter-clockwise looking upstream, deg |
| $\psi$ | Wind tunnel flow angle in yaw plane, to the right positive looking upstream, deg |
| $\omega_x$ | Vorticity component in the y-z plane, rad/sec |
| $\omega_z$ | Vorticity component in the x-y plane, rad/sec |

# CHAPTER I

# INTRODUCTION

## I. PRELIMINARY INFORMATION

Recent high performance aircraft designs have required more precise information from wind tunnel investigations. Modern combat aircraft designs, for instance, operating on smaller static margins and flying at wider ranges of attitude, require more precise wind tunnel measurements as well as larger quantities of data. As a recent study (1)[1] has pointed out, significant improvements in wind tunnel instrumentation have occurred over the last several years, resulting in higher accuracies of measurement. Computerized testing techniques have been devised to obtain data at faster rates and over wider ranges of model attitudes and this has resulted in larger excursions of the model surfaces through the test section flow. Consequently, the simulation accuracy of wind tunnel testing has now become significantly dependent on test section flow quality.

A great deal of effort is being expended to solve problems peculiar to transonic wind tunnels. Transonic wall corrections, adaptive test section wall configurations, and "low-noise" wall designs are major areas of work.

---

[1]Numbers in parentheses refer to similarly numbered references in the Bibliography.

Recently, however, small flow angularity disturbances have been found to exist in various test units. These disturbances, which in the past have been considered to be of little consequence to testing, are now the subject of an overall flow quality improvement endeavor.

## II. STATEMENT OF THE PROBLEM

It is entirely possible that wind tunnel test section flow angularities are significantly influenced by upstream flow disturbances entering the contraction cone and nozzle. The purpose of this investigation is to experimentally determine the nature and extent to which test section flow angularity is influenced by disturbances to the stilling chamber velocity profile. Simple distortion patterns were introduced into the stilling chamber of a transonic test facility (Tunnel 1T) by the use of various flow shaping screen devices. The distortion patterns were modified into changes in the axial velocity component only, by installing a honeycomb at the inlet to the contraction fairing. The resulting influence of the various distortion patterns on the test section flow was determined by making flow angularity surveys in the test section.

A theoretical consideration of the effect of the contraction cone on the vorticity distribution generated by the stilling chamber distortion patterns was made. A potential flow analysis was used to model the flow process

in the contraction cone and nozzle. Finally, an estimate of the resulting test section flow angularity was made and compared to the experimental measurements.

## III. ORGANIZATION OF THE MANUSCRIPT

Chapters II, III, and IV are devoted to the experimental portion of the investigation. The test apparatus will be described, with details of the flow shaping devices and survey equipment, as well as the procedure used in obtaining the results. Data reduction procedures such as those devised to separate support-induced effects from tunnel flow angularity will be outlined and data uncertainties for the various parameters will be given. Experimental results will then be presented and discussed.

Chapter V will be a theoretical discussion of the flow process considered to be dominant. A short analysis and comparison with experimental results will be made.

Chapter VI will contain conclusions based upon both the experiment and the theory. Remarks and recommendations will also be made.

# CHAPTER II

# APPARATUS

## I. WIND TUNNEL

The experiments were performed at AEDC in the PWT Tunnel 1T. This tunnel is a continuous flow, nonreturn wind tunnel equipped with a two-dimensional, flexible nozzle and a plenum evacuation system. The nominal test section Mach number range is from 0.2 to 1.5. Total pressure control is not available in Tunnel 1T. The tunnel is operated at a stilling chamber total pressure of about 2850 psf with a ±5 percent variation dependent on tunnel resistance and ambient conditions. The stagnation temperature can be varied from 80 to 120°F above ambient temperature, as necessary to prevent visible condensation in the test region. The general arrangement of the tunnel and its associated equipment is shown in Figure 1.[2] A detailed description of the tunnel and its capabilities is given in (2).

## II. TEST INSTALLATION

The test installation of the various pieces of equipment for the Tunnel 1T flow angularity test is illustrated in Figure 2. The stilling chamber velocity distortion

---

[2] All figures and the table are in the Appendix.

patterns were produced by using half-plane and quarter-plane screens installed in various orientations in the upstream end of the stilling chamber. The screened panels consisted of a 40 mesh, 0.007 wire screen backed by a 6 mesh, 0.041 wire screen which produced a pressure loss factor ($\Delta p/q$) of about 2.1. The various flow shaping device configurations are outlined in Table 1.

A honeycomb structure, which consisted of a quarter-inch cell of 0.003-inch aluminum foil, 3-inch deep, was installed just downstream of the flow shaping screens. This arrangement resulted in a stilling chamber flow with various gradients imposed on the axial velocity component but with very little variation in the transverse velocity components.

For the stilling chamber survey phases of the test, a full span pitot rake with 42 pressure probes was installed approximately 7 inches upstream of the contraction fairing in the stilling chamber, as shown in Figure 2, with a mechanism for rotating the rake to prescribed angles. The velocity distribution in the stilling chamber was then determined for the various flow shaping screen configurations by rotating the mechanism and measuring variations in total pressure along the rake referenced to stilling chamber static pressure.

The arrangement for the test section surveys is also shown in Figure 2. A pressure type flow angle probe was mounted on an offset arm support attached to a roll

mechanism which was installed on the Tunnel 1T sting support system. A photograph of the test section installation is shown in Figure 3. Flow angle and Mach number survey data were taken over a 6- by 11-inch cross section of the flow at station 20.0 by vertically translating and rolling the probe support mechanism. The flow angle probe, shown in Figure 4, was calibrated in Tunnel 1T during previous technology investigations (3). It is a hemispherical tipped, 0.25-inch-diameter, pressure probe with five 0.02-inch-diameter orifices, one at the stagnation point and four on the 35-deg meridian arranged 90-deg apart. Flow angles in two orthogonal planes and local Mach number were determined using this probe.

## III. INSTRUMENTATION

Stilling chamber velocity profiles were measured using a pitot probe instrumented with a scanivalve and a 1-psi differential pressure transducer. Four equally spaced static orifices around the stilling chamber at the plane of the pitot rake were interconnected and used as a reference for the transducer. The rake was rolled to prescribed positions using a motor and chain drive system instrumented with a potentiometer which was calibrated and used to set the rake position.

Flow angularity data were obtained with a pressure type flow angle probe instrumented with five 15-psi differential transducers referenced to the tunnel plenum chamber

pressure. A roll mechanism was used for positioning the probe and was equipped with a potentiometer for position readout. The standard tunnel sting support instrumentation was used for vertical translation readout.

PWT-1T was equipped with a permanently installed, automatic, data recording system. A PDP 11-20 computer provided on-line data reduction. Reduced data were displayed on a line printer, and a high-speed paper tape punch was used to record and store raw data for off-line analysis.

# CHAPTER III

# TEST DESCRIPTION

## I. PROCEDURE

Stilling chamber velocity profiles were obtained by rolling the full span rake to various roll angles between 0-deg and 180-deg (see Figure 5a). The various screen configurations were tested with the stilling chamber rake installed to determine the velocity distortion patterns obtained with each. The stilling chamber rake was then removed, the flow angle probe installed in the test section, and the screen configurations tested again. The flow angle and Mach number surveys were performed using the method of vertical translation and roll to position the probe (see Figure 5b) which resulted in vertical traverses, laterally separated by 1/2-inch, over a 6- by 11-inch cross section of the flow. Steps were taken to carefully align the flow angle probe at zero angle of attack and frequent alignment checks were made during the flow angle surveys.

## II. DATA REDUCTION

Rake total pressures and stilling chamber static pressures were obtained and used to compute velocity profiles using the relation: $p_t - p_\infty = 1/2\ \rho V^2$. These stilling chamber velocities were then normalized with a computed average stilling chamber velocity based upon tunnel total

pressure and stilling chamber static pressure determined in the same way.

The test section flow angle and Mach number data were obtained from the pressure measurements made with the flow angle probe. The algorithm for computing flow angle and Mach number from (3) was used to reduce the pressure probe data. Flow angle data were found to have errors produced by deflections resulting from aerodynamic loads on the support system and apparent interference between the support system and the tunnel walls. Each vertical traverse consisted of data obtained at a conjugate pair of roll angles. At one roll angle the roll head and sting were above test section centerline and at the other they were below centerline. A correction procedure, similar to an "upright and inverted data" analysis, was used to correct for a majority of the errors. This correction procedure allowed the determination of the support induced flow angularity by comparing data obtained with the probe tip on the tunnel centerline while the support mechanism was in both "upright" and "inverted" positions. To correct for apparent "air-on" deflections, both halves of a given vertical survey were adjusted to obtain agreement in the region of data overlap to provide continuous data profiles for each survey location. This correction procedure was used for all flow angle data, and no correction was attempted for the remainder of the errors since comparative data analysis was sufficient and the effects were present at all conditions. The comparative

data analysis approach consisted of selecting the unobstructed stilling chamber case as the baseline and calculating flow angularity for all other configurations as the difference between the baseline and the configuration of interest. The correction procedures were somewhat artificial since exact determinations of the various errors were not possible. The results of the experiment, however, were not dependent on highly precise values of the flow angularities. A general indication of the nature of the flow patterns was sufficient.

## III. DATA UNCERTAINTIES

An estimate of the uncertainties (bands which included 95 percent of the calibration data) of the basic tunnel parameters (free-stream total pressure, $p_t$, total temperature, $T_t$, and free-stream Mach number, $M_\infty$) was made from repeat calibrations of the instrumentation and from the repeatability and uniformity of the test section flow during tunnel calibration. These estimates were then used to compute estimated uncertainties of other free-stream properties (free-stream static pressure, $p_\infty$, and free-stream dynamic pressure, $q_\infty$) using the Taylor series method of error propagation. The estimated uncertainties thus obtained are given below:

| $M_\infty$ | $\Delta M_\infty$ | $\Delta P_t$, psf | $\Delta T_t$, °F | $\Delta p_\infty$, psf | $\Delta q_\infty$, psf |
|---|---|---|---|---|---|
| 0.6 | ±0.003 | ±5.5 | ±4.1 | ±6.8 | ±5.8 |

The uncertainty of the stilling chamber velocity measurements was calculated based on the instrumentation uncertainties and was found to be ±2.4 ft/sec. The calculated uncertainty of the nondimensional stilling chamber velocity, $V/V_A$, was found to be ±0.066. Uncertainties in the measurements made with the flow angle probe were used to calculate the uncertainties in the measured probe parameters (Mach number and flow angle) which are given below:

| ΔMP | $\Delta\alpha$, deg | $\Delta\psi$, deg |
|---|---|---|
| ±0.004 | ±0.05 | ±0.05 |

The roll mechanism was found to have appreciable internal play which resulted in some "air-on" angular deflections as previously mentioned.

Positional accuracy of the stilling chamber rake readout system was within ±0.1 deg in roll, and the lateral and vertical accuracy of the flow angle probe was estimated to be within ±0.1 inch.

# CHAPTER IV

## EXPERIMENTAL RESULTS

### I. STILLING CHAMBER VELOCITY PROFILES

Selected stilling chamber velocity profiles are shown in Figures 6 through 8 for the various screen configurations. Normalized velocity is presented versus the rake coordinate (L) at a series of rake roll angles ($0° \leq \phi_R \leq 180°$) for each configuration. Note that at a roll angle of zero, the data near the bottom of the stilling chamber are at negative values of L. Reference should be made to the nomenclature described in Figure 5a to avoid confusion when considering the stilling chamber velocity data.

Velocity profiles for the unobstructed stilling chamber are shown in Figure 6. These data illustrate a velocity distribution with no gross distortion, however, it should be pointed out that the flow was highly dynamic and the disturbances shown are an instantaneous representation of the dynamic profile variation. Each data point represents the average of three values. The dynamics resulted mainly from the upstream valve configuration and the close proximity of the compressor exit. All of the test data were obtained with heavy turbulence screens installed in the valve exit in an effort to flatten the stilling chamber

profile and minimize flow dynamics.

Velocity profiles for the half-plane distortion screen arranged in the lower half of the stilling chamber (screen configuration 1) are shown in Figure 7. These data illustrate a simple step change in velocity between upper and lower halves of the stilling chamber. The disturbances in the profile, which are an indication of the dynamic nature of the flow, seem to be greater in the lower velocity region. The velocity change produced by the screen is about a 40 percent reduction over half the stilling chamber flow. The half-plane screen was arranged in three other orthogonal orientations in the stilling chamber (configurations 2 through 4) and the resulting velocity distribution was surveyed. In general, the same comments apply for these configurations as for the configuration 1 except that the high and low velocity regions geometrically correspond to the position of each screen within the stilling chamber.

A quarter-plane screen was also tested. The velocity distribution obtained with this screen in the lower right quadrant of the stilling chamber (configuration 5) is illustrated in Figure 8. These data indicate a somewhat smaller velocity change between the obstructed and unobstructed regions of the flow than was experienced with the half-plane screen. A decrease in velocity of about 30 percent is typical. Similar disturbances to those found with the half-plane screen installed, indicating flow

fluctuations, exist in the velocity profiles obtained with the quarter-plane screen. Examination of the data obtained with the quarter-plane screen installed in two other quadrants of the stilling chamber, lower left (configuration 6), and the upper right (configuration 7), reveal essentially the same velocity distribution compatible with each screen orientation.

## II. TEST SECTION MACH NUMBER PROFILES

Test section Mach number profiles were obtained at $M_\infty = 0.6$ for all stilling chamber screen configurations simultaneously with flow angle data. Typical results are shown in Figure 9 for the vertical centerline at test section station 20.0. It is readily seen that no gross disturbance in the profile exists as a result of the presence of screen configurations 1 and 2 in the stilling chamber and these results are typical of all configurations. The test section data did not exhibit the dynamic disturbances noted in the stilling chamber measurements. Differences in the boundary layer are noted in these data, however, the relationship of the boundary layer thickness to screen configuration is not considered here.

## III. TEST SECTION FLOW ANGULARITY DISTRIBUTIONS

Flow angularity surveys were made in the Tunnel 1T test section at station 20.0 with the various screen

configurations installed in the stilling chamber.

Surveys for the open stilling chamber case are shown in Figure 10. These data reveal a general increase in pitch and yaw angle with increasing distance from the vertical centerline survey. It was concluded, as previously stated, that the apparent increase in flow angles with lateral distances are a result of support deflections and aerodynamic interference. Variations in the data, other than that just cited, seem to be minor in nature, except near the walls, indicating that no major flow angle disturbances are present with this tunnel configuration. Corrections were obtained, as pointed out, from the data of Figure 10 and applied to the data obtained for the other stilling chamber screen configurations. These corrected data are not presented here in the form of Figure 10, however, further discussion is reserved for later figures. In general, the data reveal significant changes in flow angles. With the various screen configuration changes and, in cases where geometrically opposite screens are compared, opposite flow angle trends are noted except for a specific instance cited below.

The stilling chamber screens were fixed in place using a cruciform brace to provide structural integrity. This brace assembly consisted of 3/8-inch thick steel cross members with a 2-inch chord and chamfered leading edges. The screens were affixed to the downstream edge of this brace. It was desired to assess the effect, if any, of the

brace alone on test section flow angularity. The data of Figure 11 illustrate the results of the presence of the brace assembly in the stilling chamber. Comparison of these data to the data of Figure 10 reveals the extent of influence the rather streamlined brace had on test section flow angularity. The data of Figure 11 are uncorrected to facilitate direct comparison with the data of Figure 10. It can be noted that some disturbances are present off centerline, however, the largest disturbance appears on the vertical centerline. This is a significant trend consisting of an upwash below tunnel centerline and a downwash above. This same trend was noted in the data for the various screen configurations except for the half-plane screen mounted in either the left or right half of the stilling chamber, configurations 3 and 4, respectively.

Vector diagrams of the pitch and yaw flow angles at each point in the flow were prepared for each screen configuration from the data profiles obtained. The diagram for screen configuration 1 is shown in Figure 12. The data of Figure 12 reveal very large flow angles existing near the top and bottom walls. Also notable is the upwash and downwash existing on the vertical centerline which, as pointed out, is a probable effect of the cruciform brace. The distribution, in general, reveals a pattern having an upwash on the tunnel centerline and a downwash near the sidewalls near z equal to zero. Note that the sidewalls exist at y = ±6-inch and that the vector diagram extends only to y = ±4-inch.

Flow angle vectors are presented in Figure 13 for screen configuration 2. This configuration is geometrically opposite of the previous one and the resulting test section flow angularity pattern generally exhibits opposite trends. Similar comments apply to the data of this figure as were made for the previous figure with regard to disturbances near the upper and lower walls. The essential characteristic illustrated here is the reversal of the previous pattern, that is, the apparent downwash on the tunnel centerline with an upwash existing near the sidewalls. The results with the half-plane screen oriented in the right half of the stilling chamber are shown in Figure 14. It is readily apparent that the pattern seen in the previous figures is again present in this one and it is, again, aligned with the screen orientation. The crossflow, right to left is clearly visible on the tunnel centerline with the opposite flow direction existing near top and bottom walls. The effect of the cruciform brace is not present on the vertical centerline, however, indications of a similar effect are noted on the horizontal centerline. The data of Figure 15 illustrate the results of screen configuration 4. These vectors describe an almost identical but opposite pattern as was noted for the previous configuration. The flow angularity results for this series of half-plane screen configurations clearly show a pattern consistent with screen orientation in the stilling chamber. Further, review of the vector plots for the half-plane

screens show a possible counter rotating swirl flow producing a crossflow near centerline emanating from the low velocity region of the stilling chamber with opposite crossflows nearer the walls.

The flow angle vector diagram for the quarter-plane screen, configuration 5, is shown in Figure 16. These data illustrate a somewhat more complicated result than was found with the half-plane screens. The most notable features of the flow pattern are a crossflow from right to left just below centerline, $y = 0$, and opposite crossflows existing near the bottom wall and above centerline. Screen configuration 6 results in a very similar flow angularity pattern to the previous one except that it is symmetrically reversed about the vertical centerline (Figure 17). Some differences exist in the distributions, however, the same general pattern is evident. A final quarter-plane screen, configuration 7, was tested and the resulting flow angle patterns are illustrated in Figure 18. The similarity with the previous two distributions is noted. The pattern is essentially the same as the one of Figure 16 (configuration 5), except for being reversed about the horizontal centerline. In all three cases with the quarter-plane screen configurations the resulting flow angle pattern was consistent with screen orientation. The data revealed that, although more complicated, the flow pattern with the quarter-plane screen gave evidence of a crossflow emanating from the region of low velocity in the

stilling chamber with adjacent crossflows of opposite direction.

# CHAPTER V

## THEORETICAL CONSIDERATIONS

### I. VORTICITY DISTRIBUTION

During the experimental investigation it was understood that velocity distortions in the stilling chamber would affect test section flow angularity, however, the nature of the process by which this took place was not clear. Scorer (4), in a discussion of vorticity in natural phenomenon, described the flow process which results in circulation in the wake of tree trunks. An illustration is given in Figure 19 which describes the distortion of the boundary layer generated vorticity as it encounters the tree trunk. The lines of vorticity bend around the tree to become nearly parallel in the wake and produce counter rotating swirls. An excellent illustration of this sort of flow is the curvature of snow drifts that form around a tree trunk or other obstacles subjected to drifting snow. This concept became the seed for the development of the current understanding of the flow process existing in the wind tunnel.

The effect of the contraction fairing became important in light of Scorer's physical concept. Stilling chamber velocity disturbances can be represented as distributions of vorticity and the distortion of these lines of vorticity as the flow proceeds through the contraction

fairing could clearly be responsible for the experimental results obtained. Two basic vorticity concepts outlined by Sommerfeld (5) are pertinent to the discussion: a) vortex lines or tubes must end at a fluid boundary or proceed to infinity and b) vorticity is convective, that is, remains associated with the fluid particles. These, of course, are inviscid concepts which are also considered descriptive of the flow behavior in the free stream of the present experiment. An attempt was then made to describe the specific effect the Tunnel 1T contraction had on the vorticity generated by the flow shaping devices.

## II. CONTRACTION AND NOZZLE FLOW MODEL

The vorticity generated by the half-plane screens, for instance, exists as a sheet of vortex lines transverse to the flow direction in the stilling chamber. It was important to obtain an estimate of the change in shape of these lines as they moved with the associated fluid particles through the contraction fairing and nozzle. A potential flow model utilizing the vortex lattice technique had already been developed by Palko (6) to study the flow through a contraction and nozzle geometry very similar to the Tunnel 1T design. A streamline calculation had been made by Heltsley (7) using this model and those results were used in the present study to compute the arrangement of a line of fluid particles which initially was straight and transverse to the direction

of flow and then which flowed through the contraction and nozzle. Illustrated in Figure 20 is a two-dimensional representation of the contraction and nozzle with the streamline pattern obtained by Heltsley and the results of the computations of the fluid particle displacements based upon the streamline velocities. It is important to note the degree to which the line of fluid particles (and thereby vorticity) has been distorted when it reaches the test section. Some elements of the line are almost parallel to the flow direction rather than transverse to it as they initially were in the stilling chamber. It is clearer from the illustration of Figure 21 that the inviscid analysis gives evidence of the presence of a counter-rotating pair of swirls in the test section. The process is very similar to the example of the snow drift around the tree. Lines of vorticity in the shear layer produced by the distortion screens are reoriented by the contraction fairing so that some elements of these lines are almost parallel to the flow direction. Since two portions of a given line become nearly parallel to the flow, one on each side of the tunnel, and each region has vorticity in the opposite direction from the other, a counter-rotating swirl develops. Further, the direction of the measured flow angularities and those expected from the reoriented line of vorticity are consistent. With a half-plane screen located in the right half of the stilling chamber, for instance, the resulting vorticity

would have a positive sense (right hand rule). As the contraction fairing accelerates the core flow faster than the flow near the walls, the line of vorticity is reoriented so that the vorticity in the lower half of the flow is positive with respect to the downstream direction and that in the upper half of the flow is negative. This is responsible for the negative crossflow on the centerline and positive crossflow near the walls measured with configuration 3 (Figure 14) in the experiment. No estimate was made of the mutual influence of the two nearly parallel portions of the line of vorticity since it is probable that this effect is negligible.

## III. COMPARATIVE RESULTS

An estimate of the magnitude of the flow angularity which could be expected in the test section from the strength of the vorticity produced by a half-plane screen in the stilling chamber was made following the physical reasoning just developed. Data obtained with the half-plane screen mounted in the right side of the stilling chamber are illustrated in Figure 22. Stilling chamber velocity data were used to determine the strength of the generated vorticity. In the x-y plane the vorticity component is represented by $\omega_z = \frac{\partial v}{\partial x} - \frac{\partial u}{\partial y}$. Since all crossflow velocities were assumed eliminated by the honeycomb, the vorticity is simply $\omega_z = -\frac{\partial u}{\partial y}$. An assumption of linear velocity change in the

shear layer was made for simplicity yielding $\omega_z = -\frac{\Delta u}{\Delta y} = -\frac{V_a\ (1.15 - 0.65)}{4/12}$ rad/sec. With an average velocity ($V_a$) of about 70 ft/sec in the stilling chamber, $\omega_z = -105$ rad/sec. Considering the measured test section distribution of crossflow angle, an estimate of the flow angle magnitude was made based upon the strength of the stilling chamber vorticity. These data, presented in Figure 22, illustrate a negative sidewash (to the left looking upstream) along the central four inches of the tunnel with positive sidewash components near each wall indicating counter-rotating swirls. By distributing the strength of the vorticity of the stilling chamber velocity profile over the similar region of crossflow velocity change in either the upper or lower half of the test section flow, an estimate of the flow angularity was obtained and compared to experimental values. Using an analysis similar to that used in the stilling chamber, the test section vorticity was expressed as $\omega_x = -\frac{\Delta v}{\Delta z}$, where $\Delta v$ is the difference between the crossflow velocities at the wall and on centerline. Since these crossflows are approximately equal, $\Delta v \simeq 2v_{C.L.}$ or twice the centerline crossflow velocity. The region of velocity change, $\Delta z$, is about three inches. Therefore, $v_{C.L.} = -\frac{\omega_x\ \Delta z}{2}$. Equating the vorticity strength between the stilling chamber and test section, neglecting the effect of "stretching" the vorticity, we have

$$v_{C.L.} = \frac{(-105)\,(3/12)}{2} = -\ 13.1 \text{ ft/sec.}$$

With a velocity of about 695 ft/sec ($M_\infty = 0.6$) in the test section, $\psi = \tan^{-1}\left(-\frac{13.1}{695}\right) = -1.08$ deg. In comparison to experimental results with crossflow magnitudes ranging from 0.7 deg to about 1.2 deg, the predicted value is well within reason. It should be noted, however, that the flow field in the "real" case is highly modified by the effects of viscosity. While predictions can be made for simple distortions such as the half-plane screen, more complicated disturbances would require a much more complicated analysis.

# CHAPTER VI

## SUMMARY AND CONCLUSIONS

An investigation was conducted in Tunnel 1T wherein a series of screen configurations were tested for effects on both stilling chamber and test section velocity and test section flow angularity. The purpose of the tests was to ascertain the nature of the effect of stilling chamber velocity distortions on the velocity and flow angularity of the test section flow of a transonic wind tunnel such as Tunnel 1T. The results of these tests provide the basis for the following conclusions:

1. Velocity disturbances consisting primarily of variations in axial velocity existing in the stilling chamber of a transonic wind tunnel result in significant flow angularity disturbances in the test section flow without producing measurable variations in the velocity distribution in the test section flow.
2. Flow angularity patterns were found to be consistent with screen position in the stilling chamber and generally indicated a counter rotating swirl flow with the central crossflow component emanating from low to high velocity regions in the stilling chamber.

3. Small disturbances to the stilling chamber flow such as produced by the cruciform brace assembly without screens attached were capable of inducing measurable flow angle disturbances in the test section flow.

Theoretical considerations regarding a plausible explanation of the flow process which results in the experimental findings was made. It is concluded that the vorticity inherent in the stilling chamber velocity disturbances is reoriented in other spatial directions as the flow passes through the wind tunnel contraction fairing. Furthermore, for simple stilling chamber disturbance patterns, a prediction can be made of the general flow angularity distribution expected in the test section and reasonable values of the flow angles can be estimated.

With regard to flow quality in wind tunnels, it is evident that stilling chamber honeycomb effectiveness is reduced when velocity disturbances exist. Properly designed honeycomb assemblies are effective in removing stilling chamber flow angularities, however, a flat stilling chamber velocity profile must be achieved if parallel flow is to be maintained in the test section. An investigation by Luchuk (8) supports this view. In that investigation, flow angularities were produced in the test section of a small wind tunnel by either installing stilling chamber screen devices or producing a jet of air normal to the tunnel flow direction through a stilling chamber wall orifice. Results showed that

a honeycomb installed downstream of the disturbance effectively reduced flow angularity only in the case of the air jet normal to the tunnel flow. A screen, however, installed at the same location was effective only when the velocity disturbances were present. The conclusion that both a flat stilling chamber velocity profile and parallel flow are prerequisites for good test section flow quality seems valid and should be kept in mind during wind tunnel design or improvement plans.

# BIBLIOGRAPHY

## BIBLIOGRAPHY


1. Marshner, Bernard W. and Young, Robert L., et al. "Integrating Wind Tunnels and Computers." Vols. I and II, University of Tennessee, Knoxville, Tennessee, June-August 1977.

2. Test Facilities Handbook (Tenth Edition). "Propulsion Wind Tunnel Facility, Vol. 4." Arnold Engineering Development Center, May 1974.

3. Palko, R. L. "Experimental Verification of a Transonic Test Technique for Full-Scale Inlet/Engine Systems Simulating Maneuvering Attitudes." AEDC-TR-74-80, October 1974.

4. Scorer, R. S. Natural Aerodynamics. New York: Pergamon Press, 1958.

5. Sommerfeld, Arnold. Mechanics of Deformable Bodies. New York: Academic Press, Inc., 1950.

6. Palko, R. L. "Utilization of the AEDC Three-Dimensional Potential Flow Computer Program." Vortex-Lattice Utilization. NASA SP-405, Langley Research Center Workshop, May 17-18, 1976. Pp. 127-143.

7. Heltsley, F. L. Private communication. Arnold Engineering Development Center, Arnold Air Force Station, Tennessee, December 1977.

8. Luchuk, W. Private communication. Arnold Engineering Development Center, Arnold Air Force Station, Tennessee, 1977.

# APPENDIX

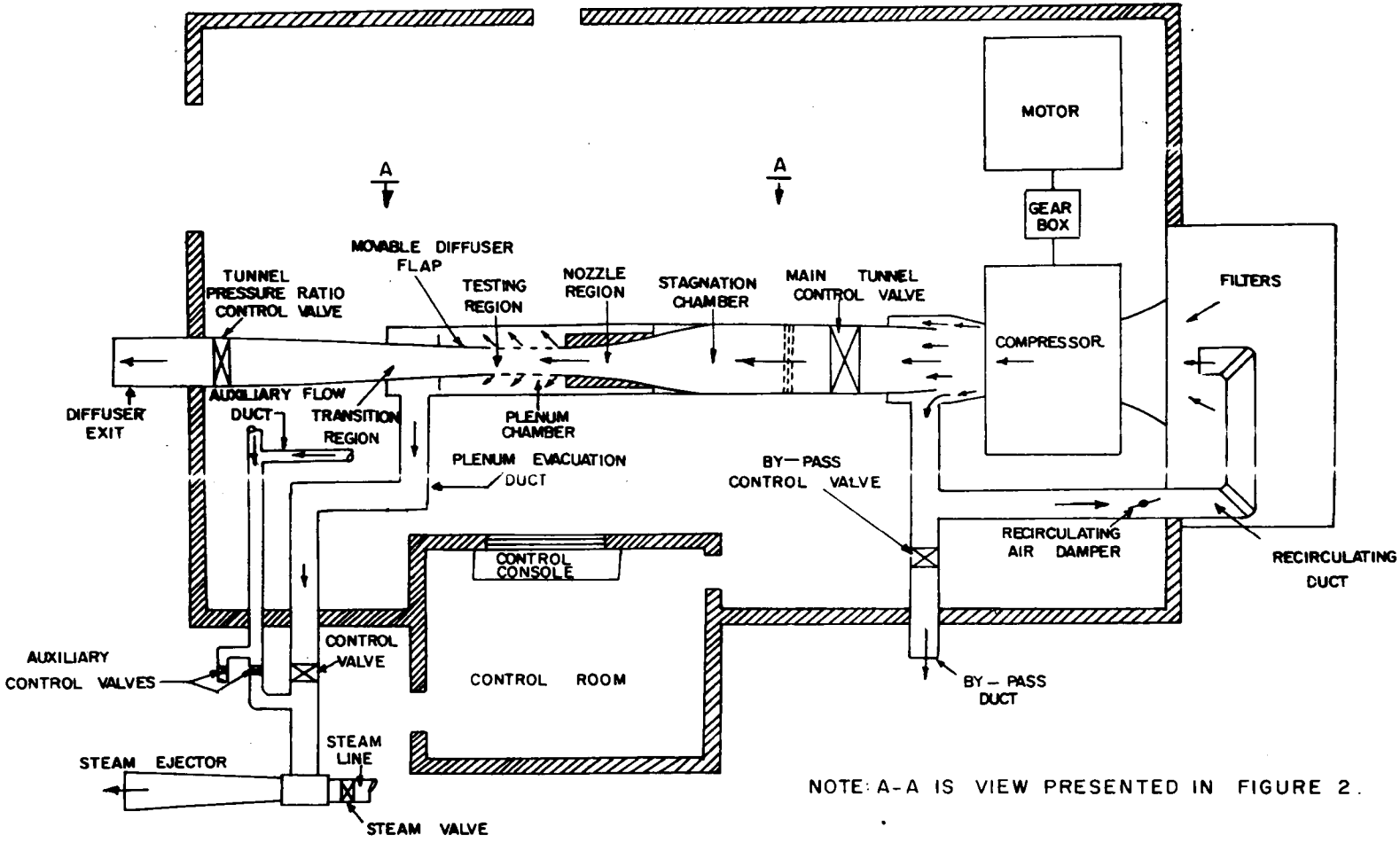



Figure 1. Schematic of Tunnel 1T and associated equipment.

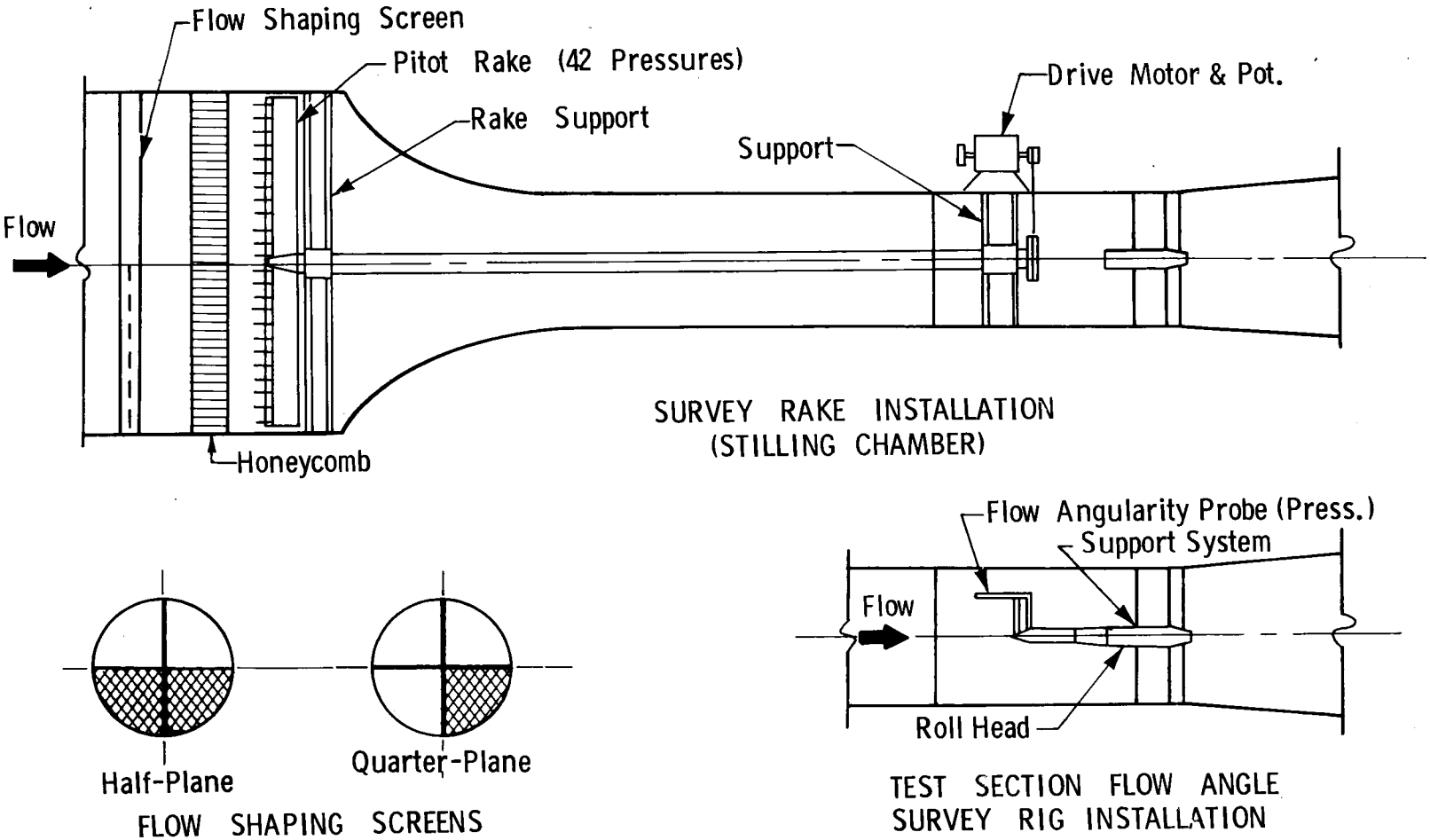



Figure 2. Schematic of test installation.

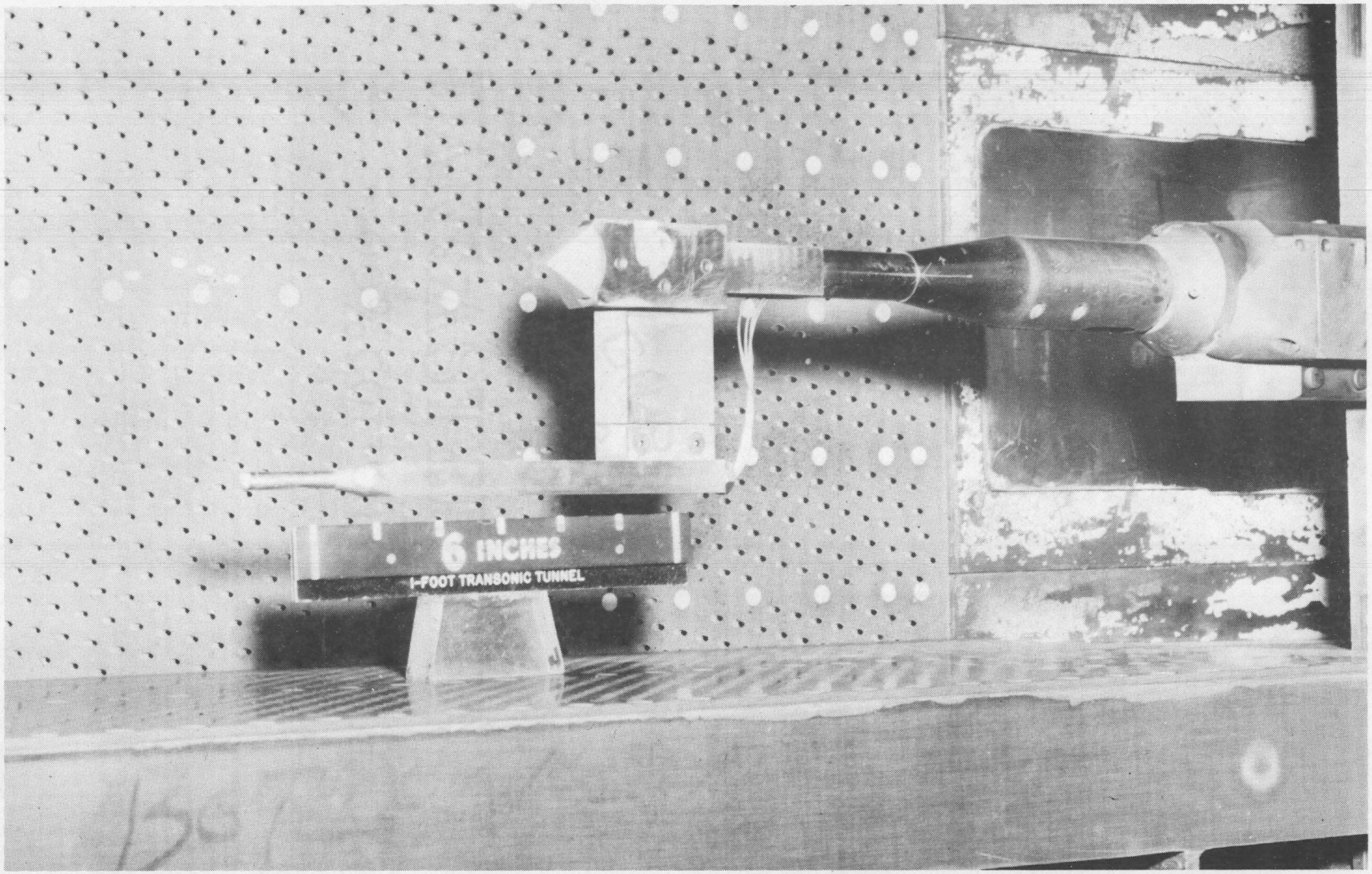



Figure 3. Photograph of flow angle probe installation.

ALL DIMENSIONS IN INCHES
UNLESS NOTED

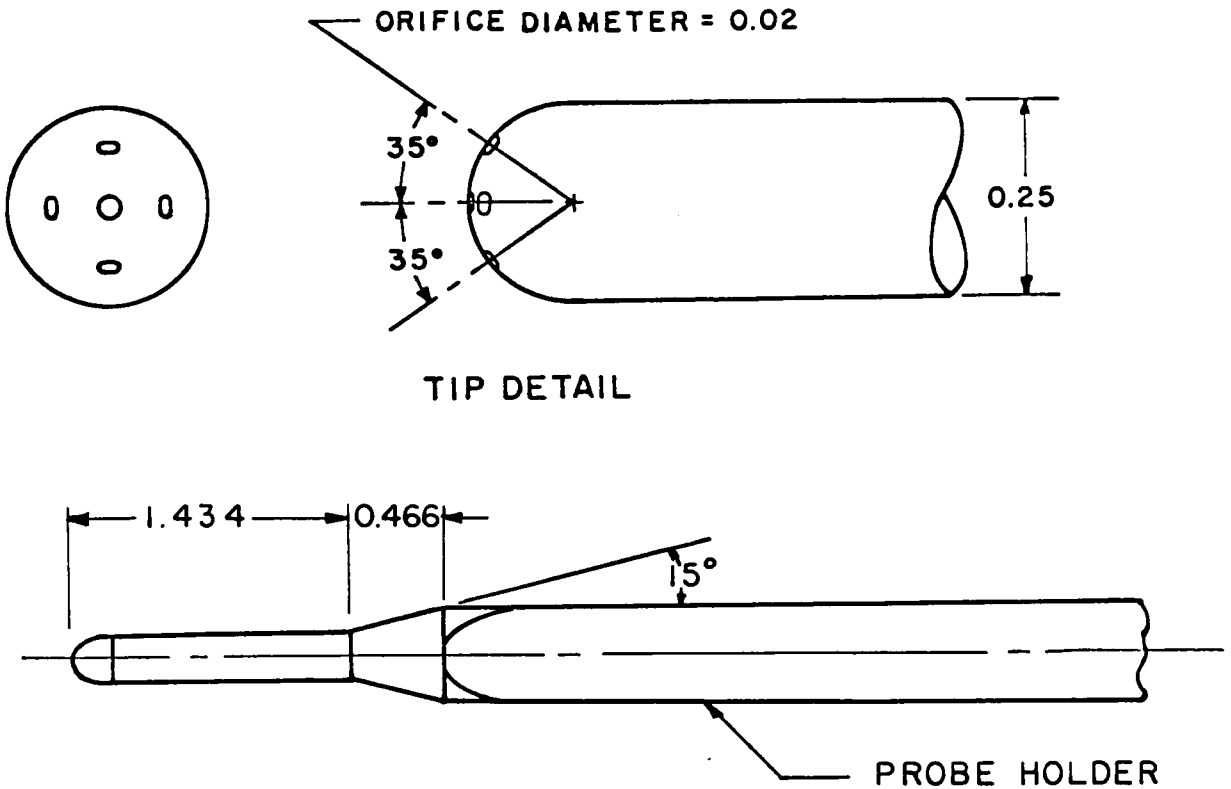
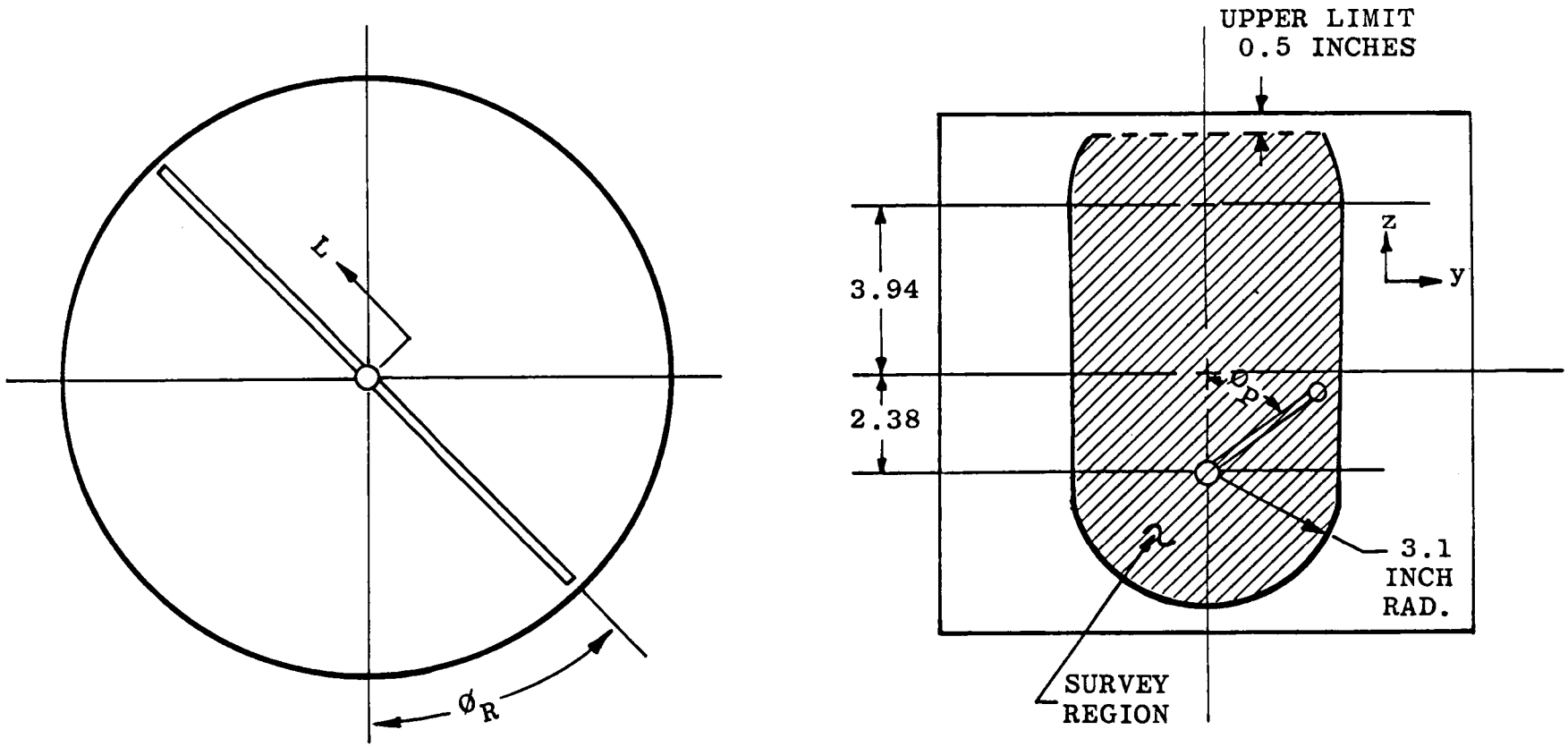


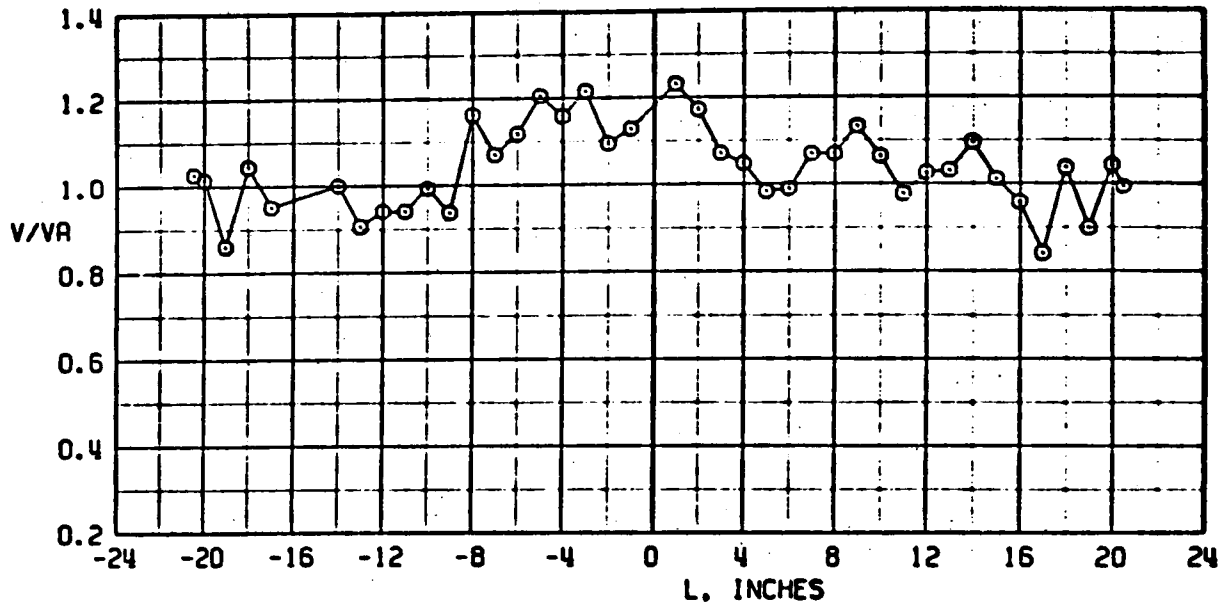

Figure 4. Details of flow angle probe.




a. Stilling chamber convention (looking upstream)

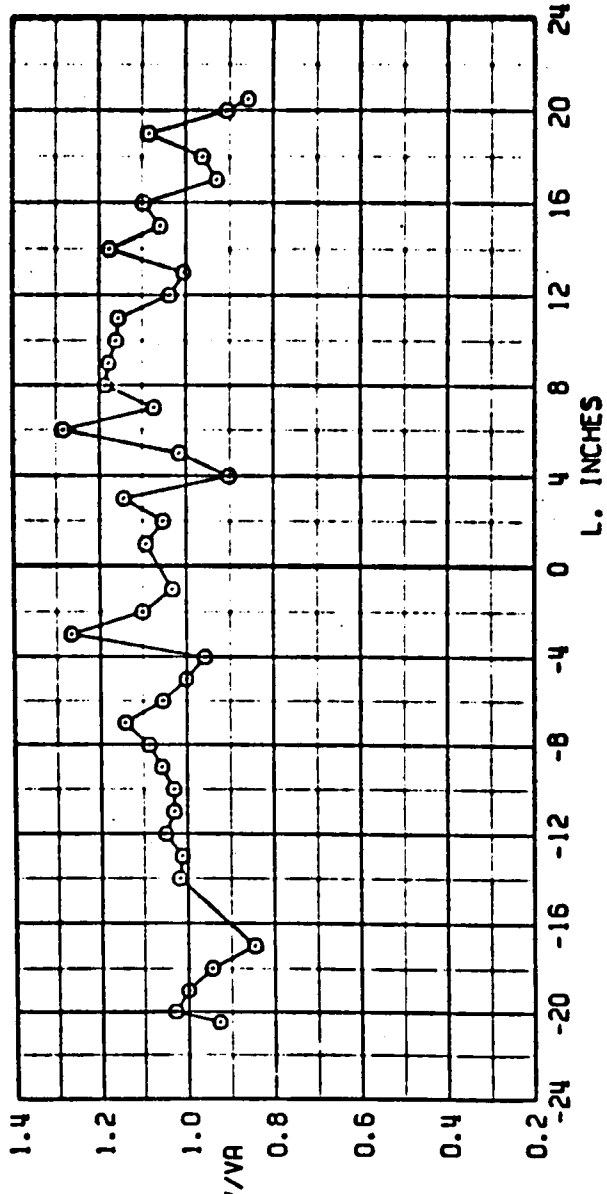
b. Test section convention (looking upstream)

Figure 5. Tunnel stilling chamber and test section nomenclature.



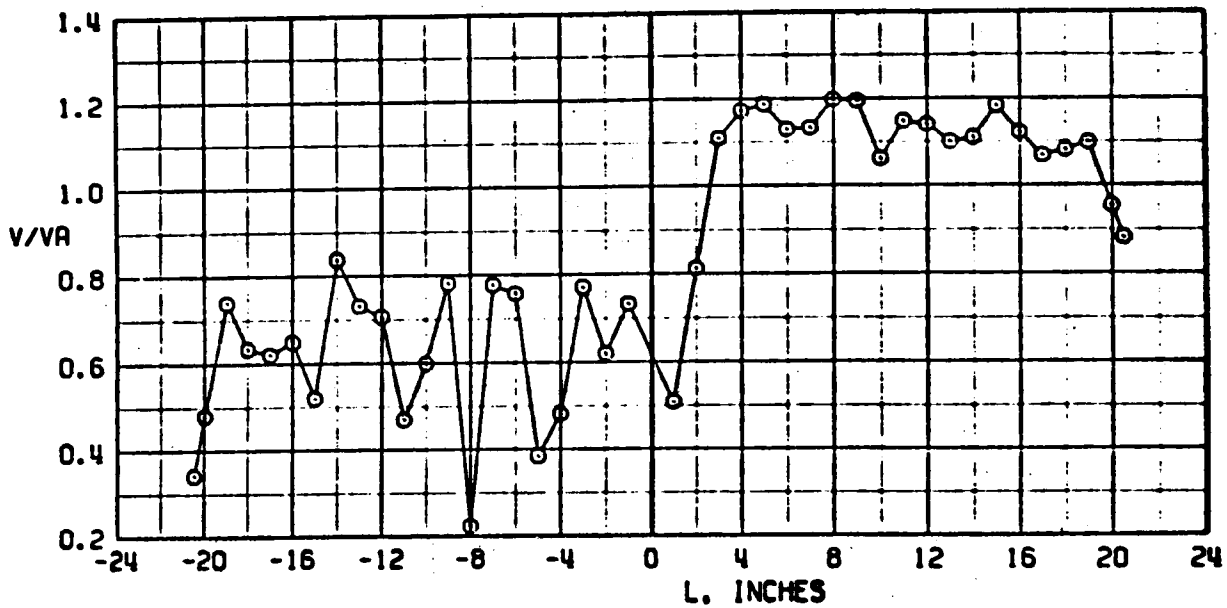

a. $\phi_R = 0$

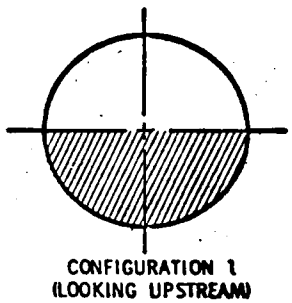
Figure 6. Stilling chamber velocity profile, open stilling chamber.




b. $\phi_R = 90$

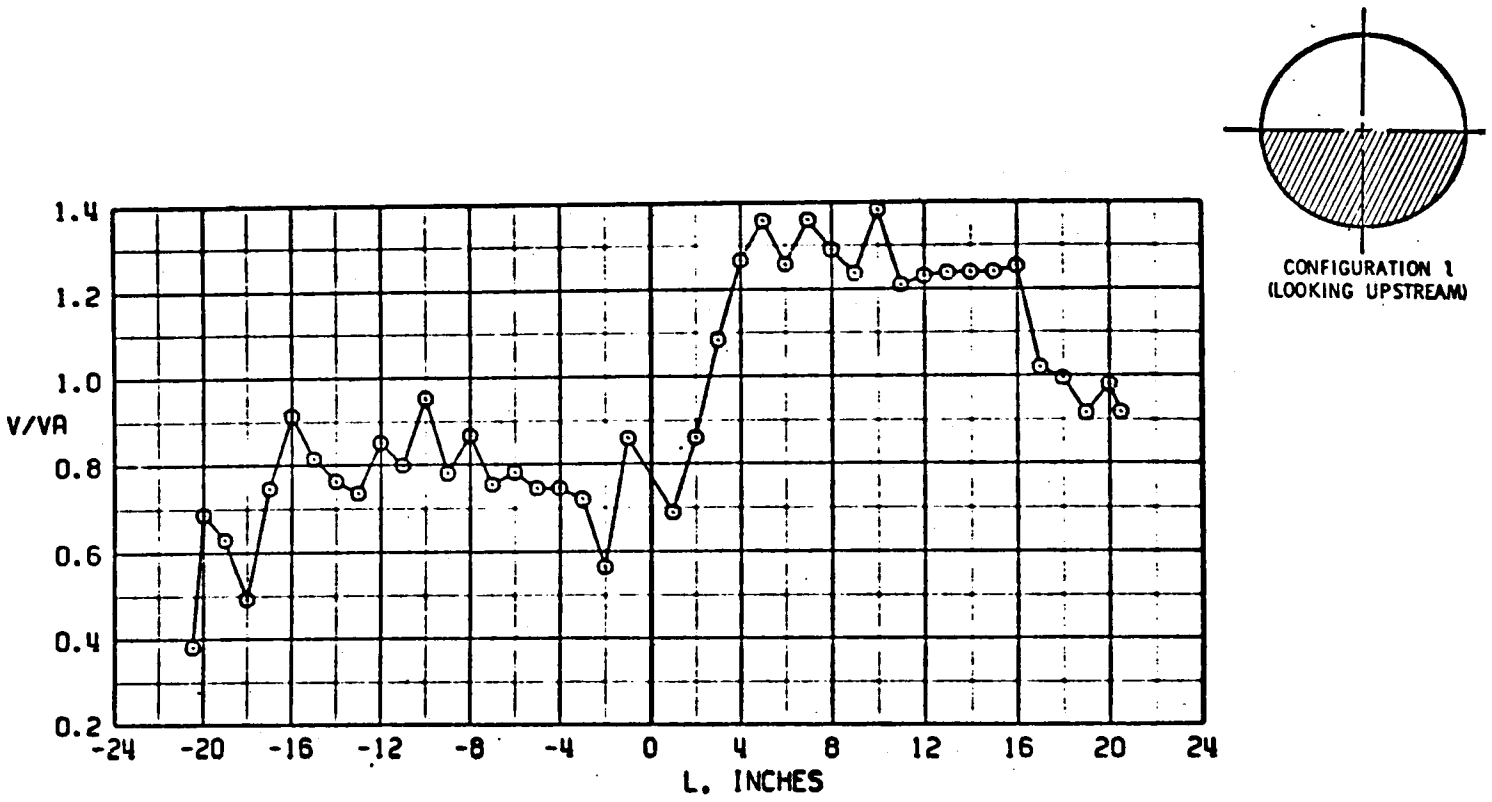
Figure 6. (Continued)



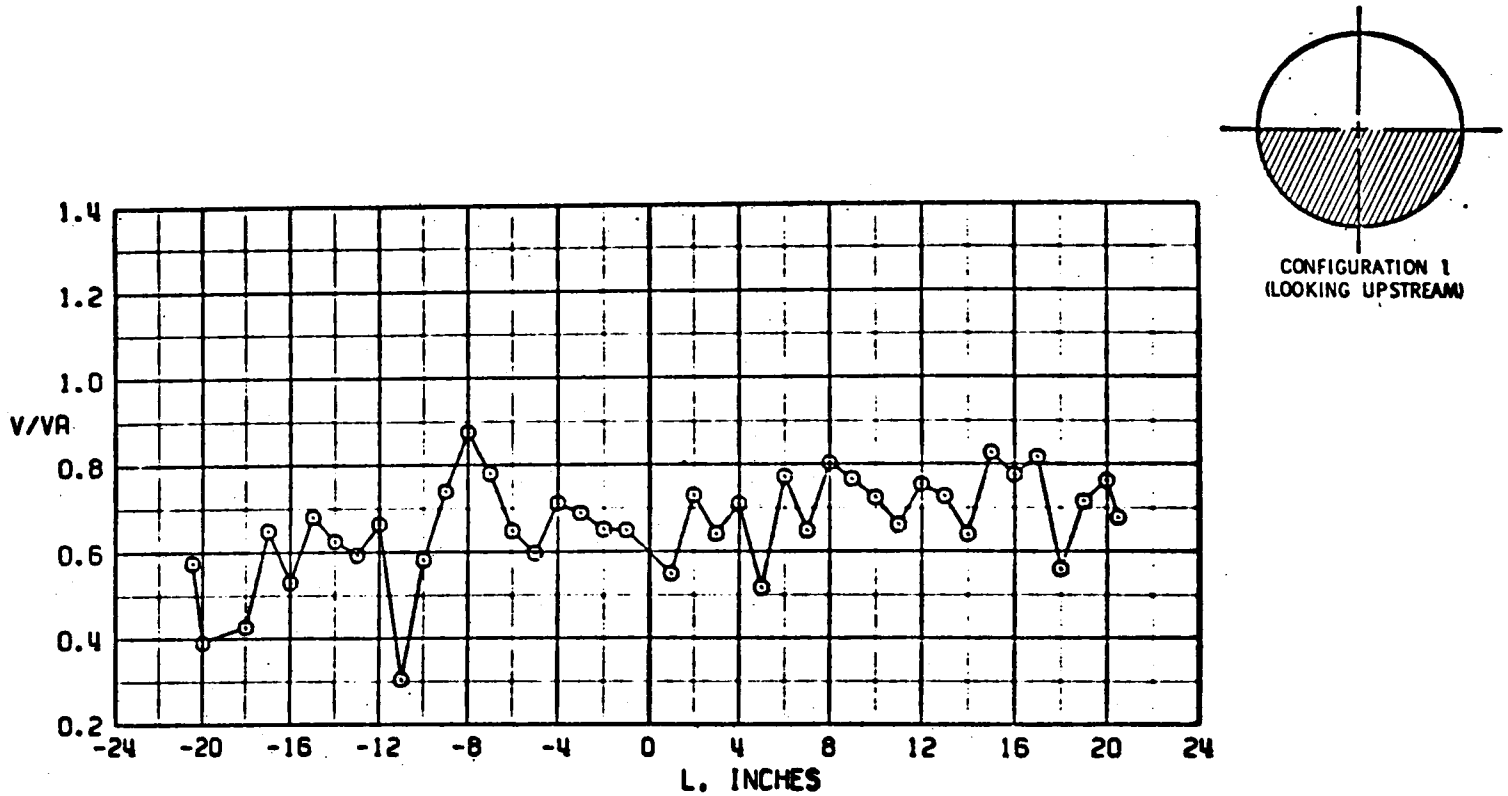

a. $\phi_R = 0$

Figure 7. Stilling chamber velocity profile, screen configuration 1.



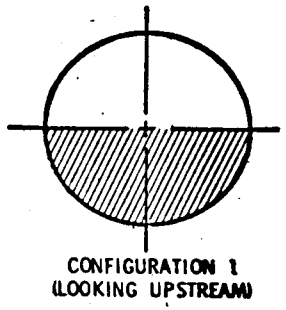

b. $\phi_R = 45$

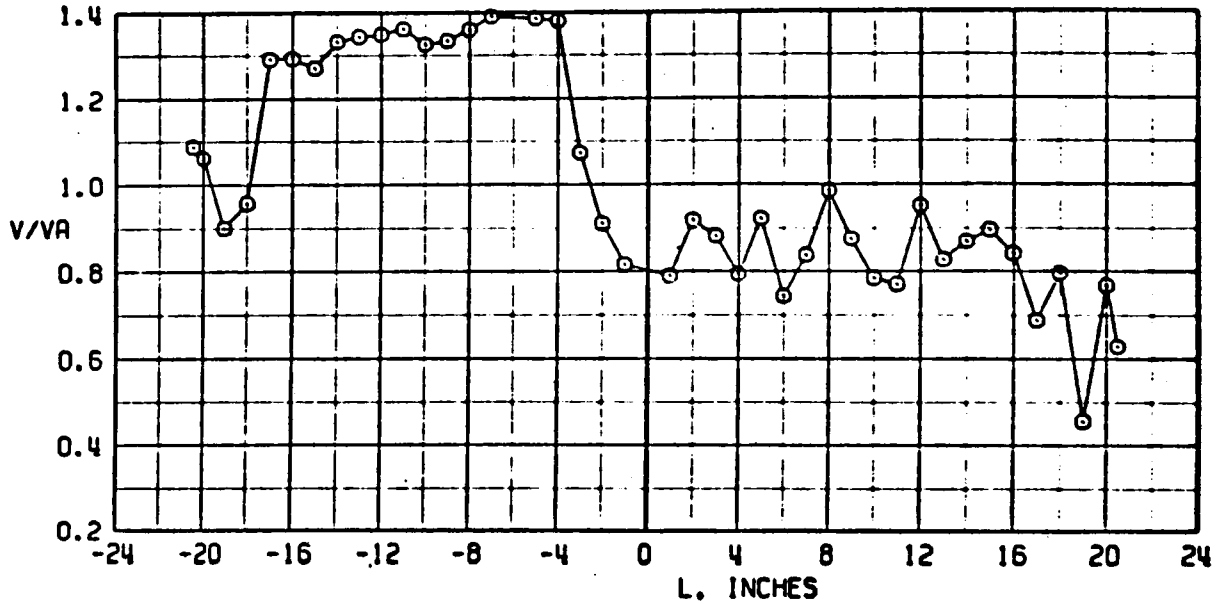
Figure 7. (Continued)




c. $\phi_R = 90$

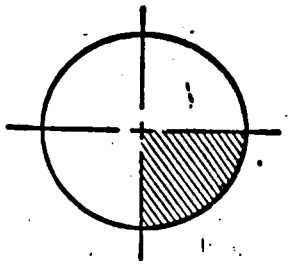
Figure 7. (Continued)

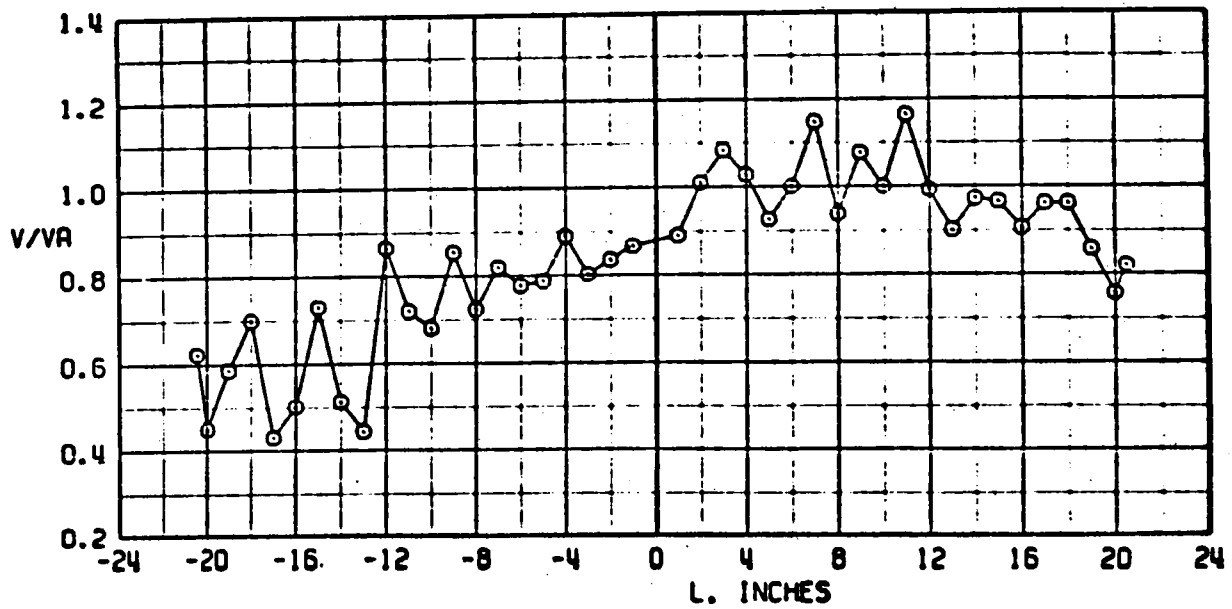



d. $\phi_R = 135$

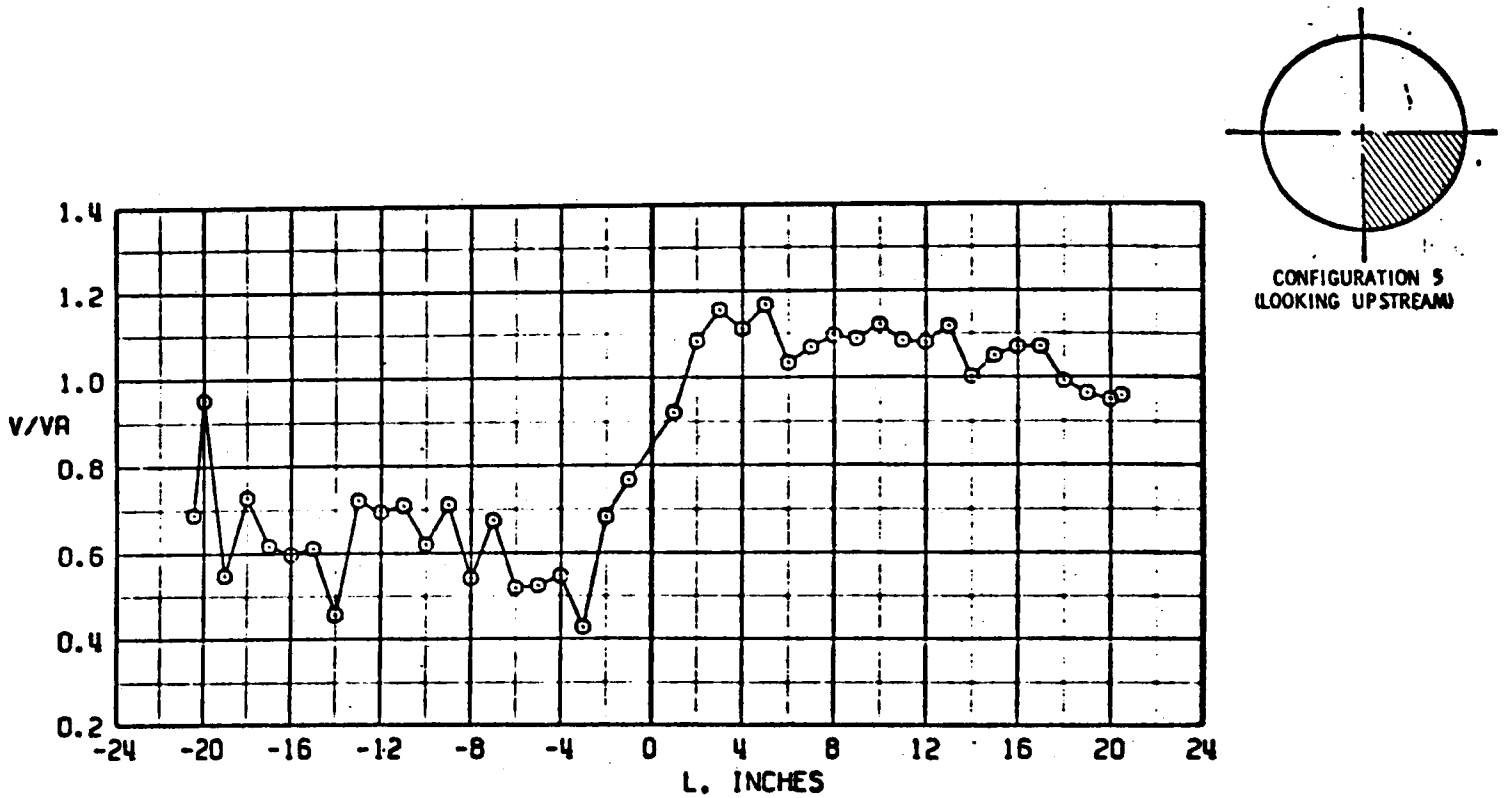
Figure 7. (Continued)



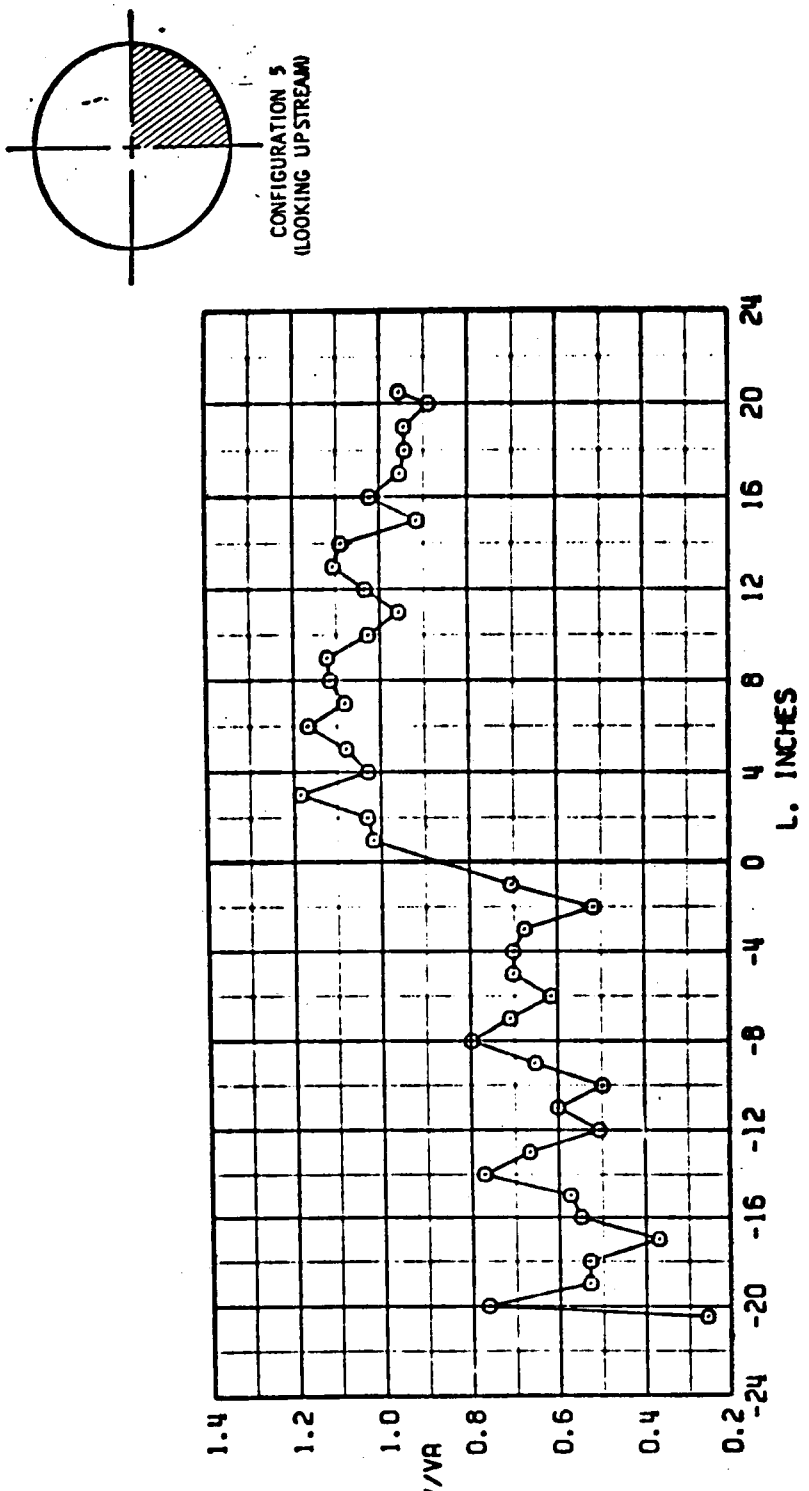

a. $\phi_R = 0$

Figure 8. Stilling chamber velocity profile, screen configuration 5.



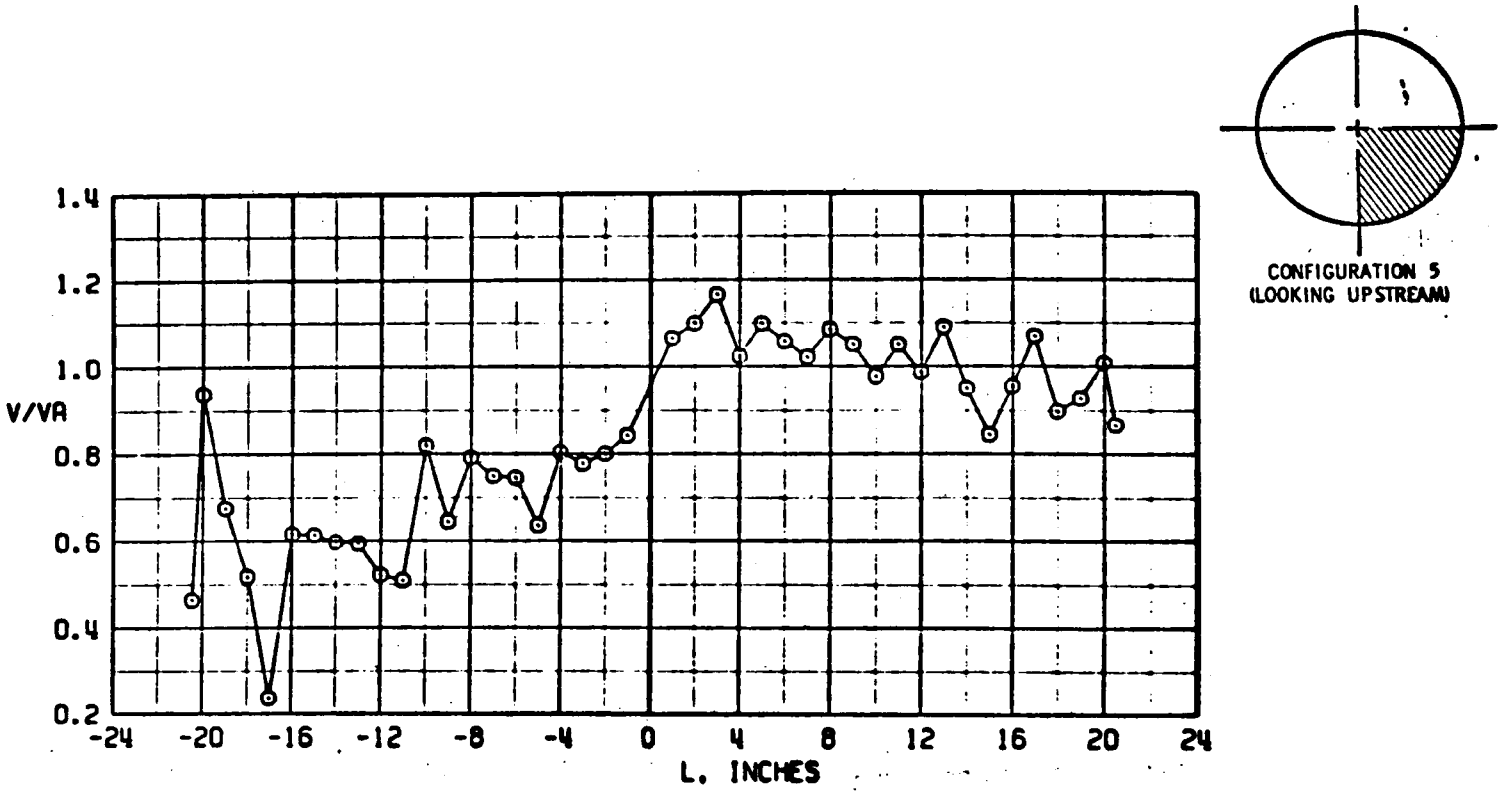

b. $\phi_R = 30$

Figure 8. (Continued)



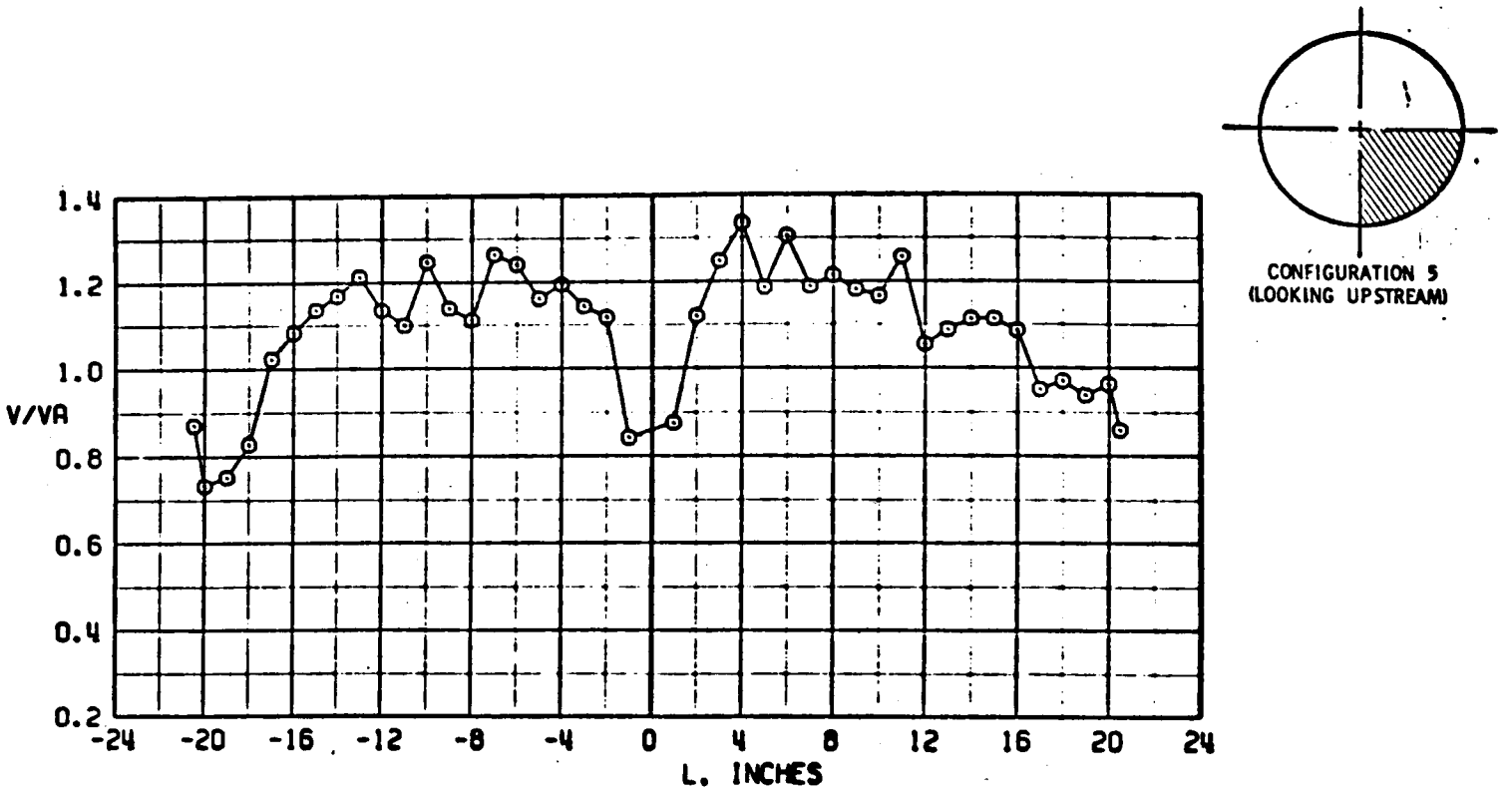

c. $\phi_R = 60$

Figure 8. (Continued)




d. $\phi_R = 90$

Figure 8. (Continued)




e. $\phi_R = 135$

Figure 8. (Continued)

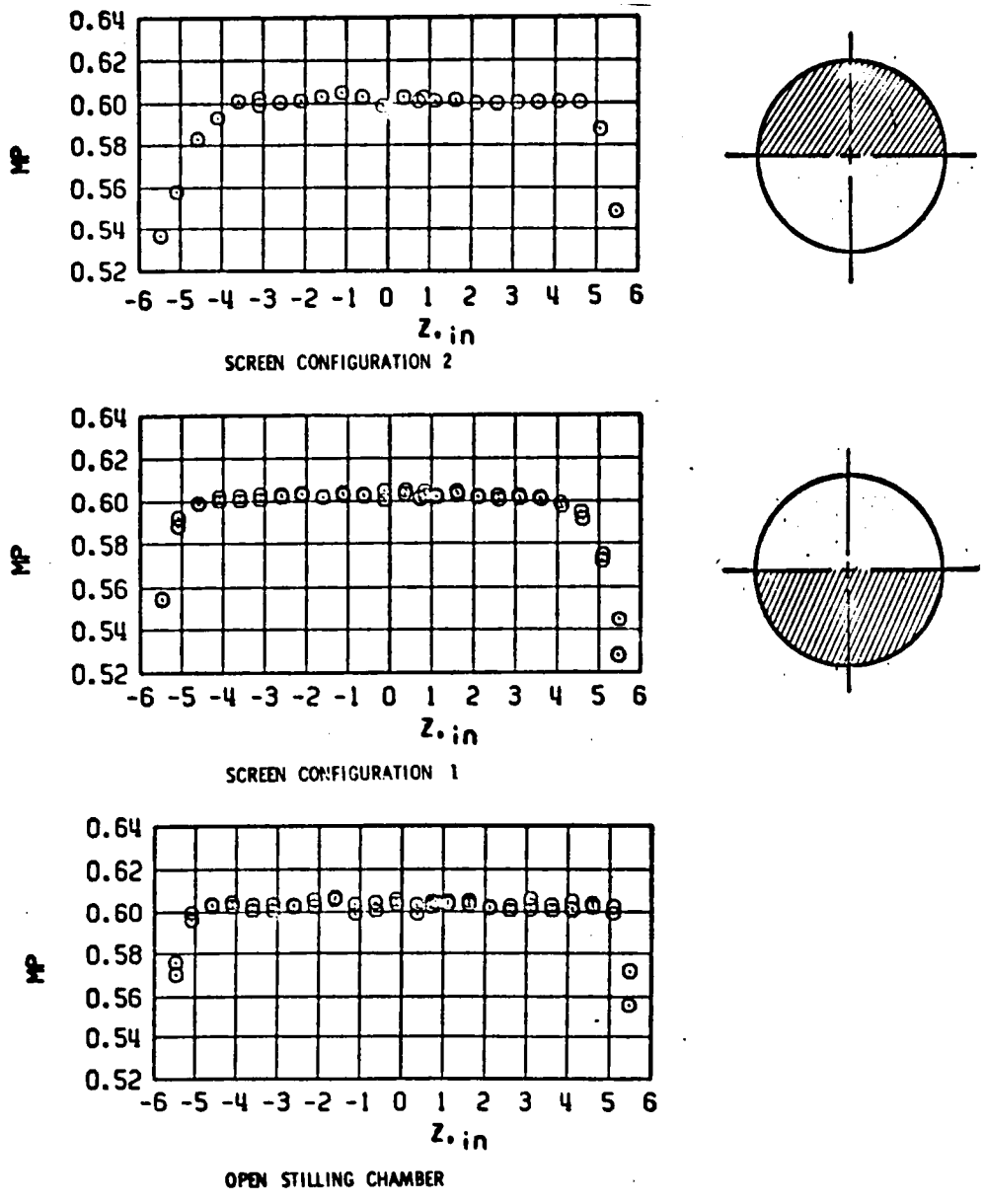
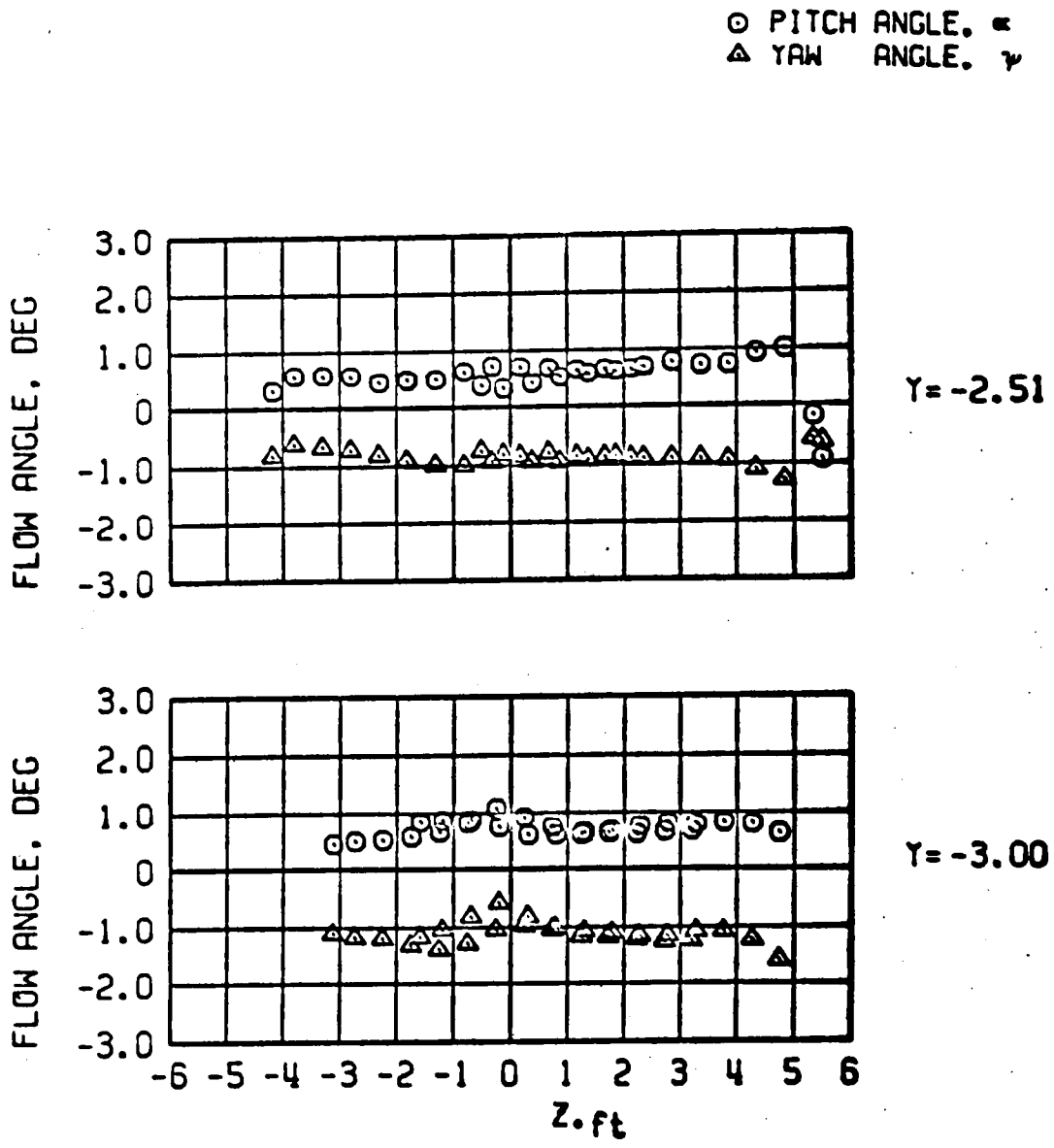
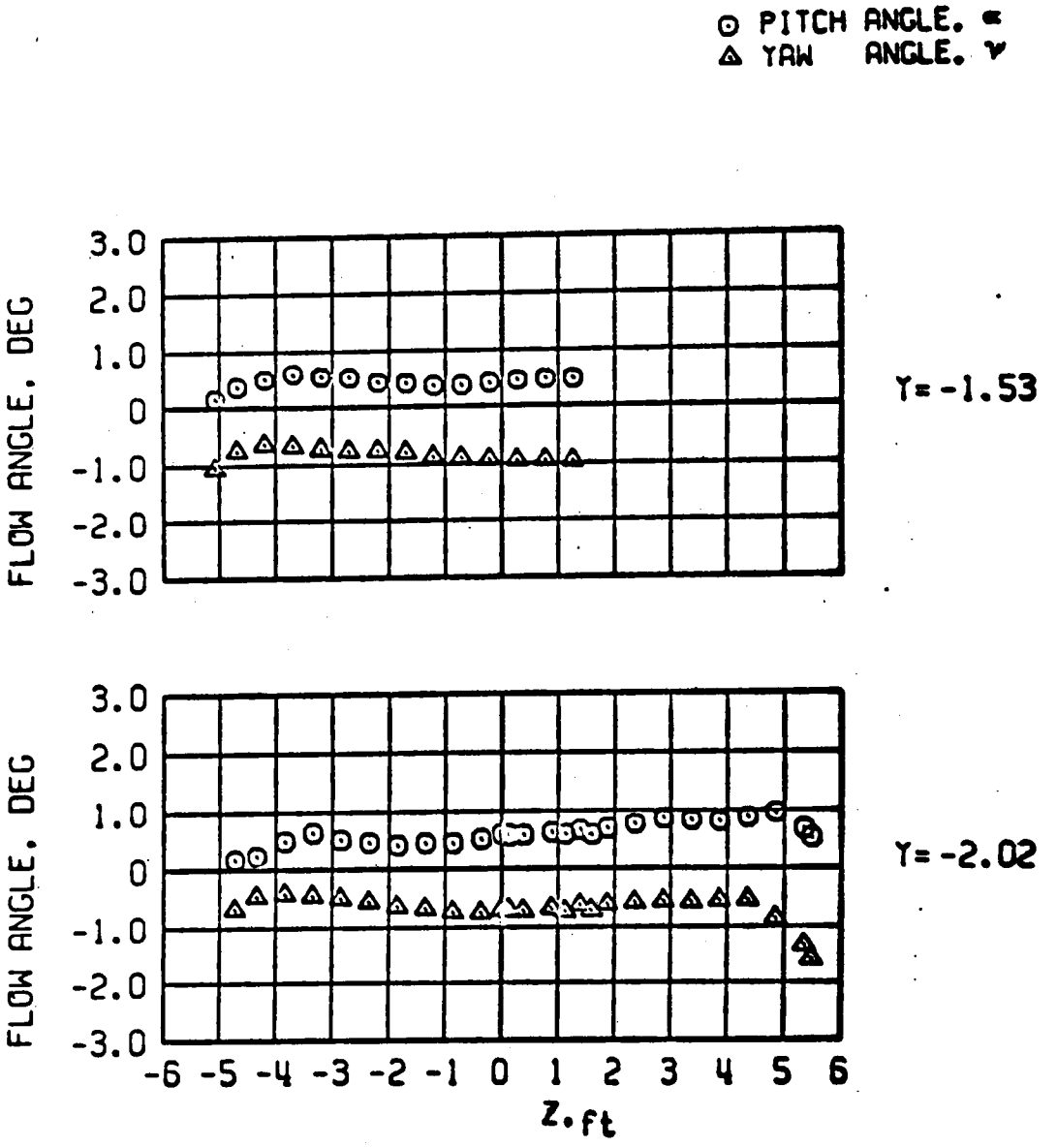



Figure 9. Test section Mach number surveys with and without screen configurations 1 and 2.



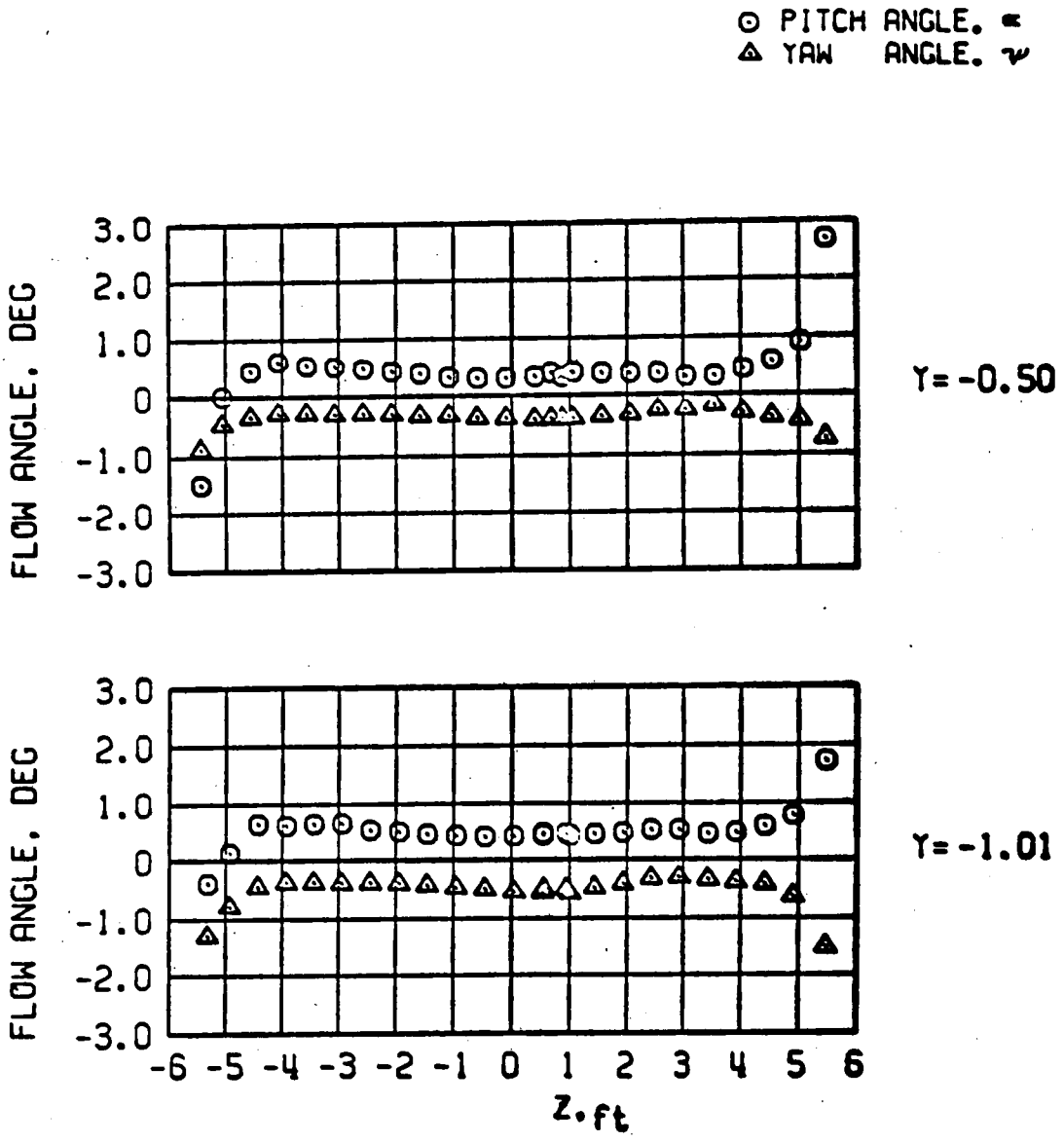

a. y = -3.0 and -2.5 inches

Figure 10. The variation of test section flow angularity with vertical position (z) at various lateral (y) positions for the open stilling chamber configuration at $M_\infty$ = 0.6.



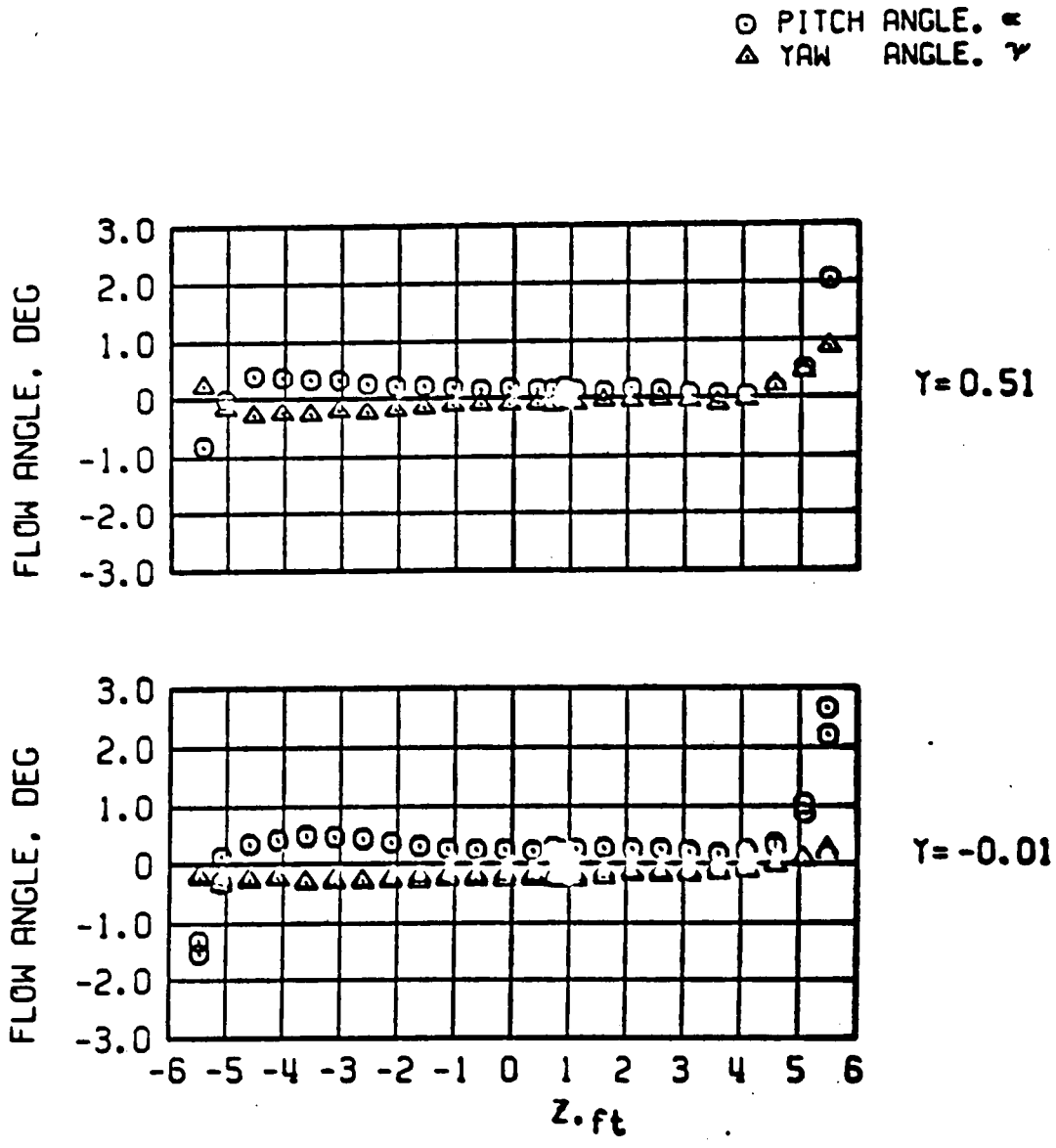

b. y = -2.0 and -1.5 inches

Figure 10. (Continued)



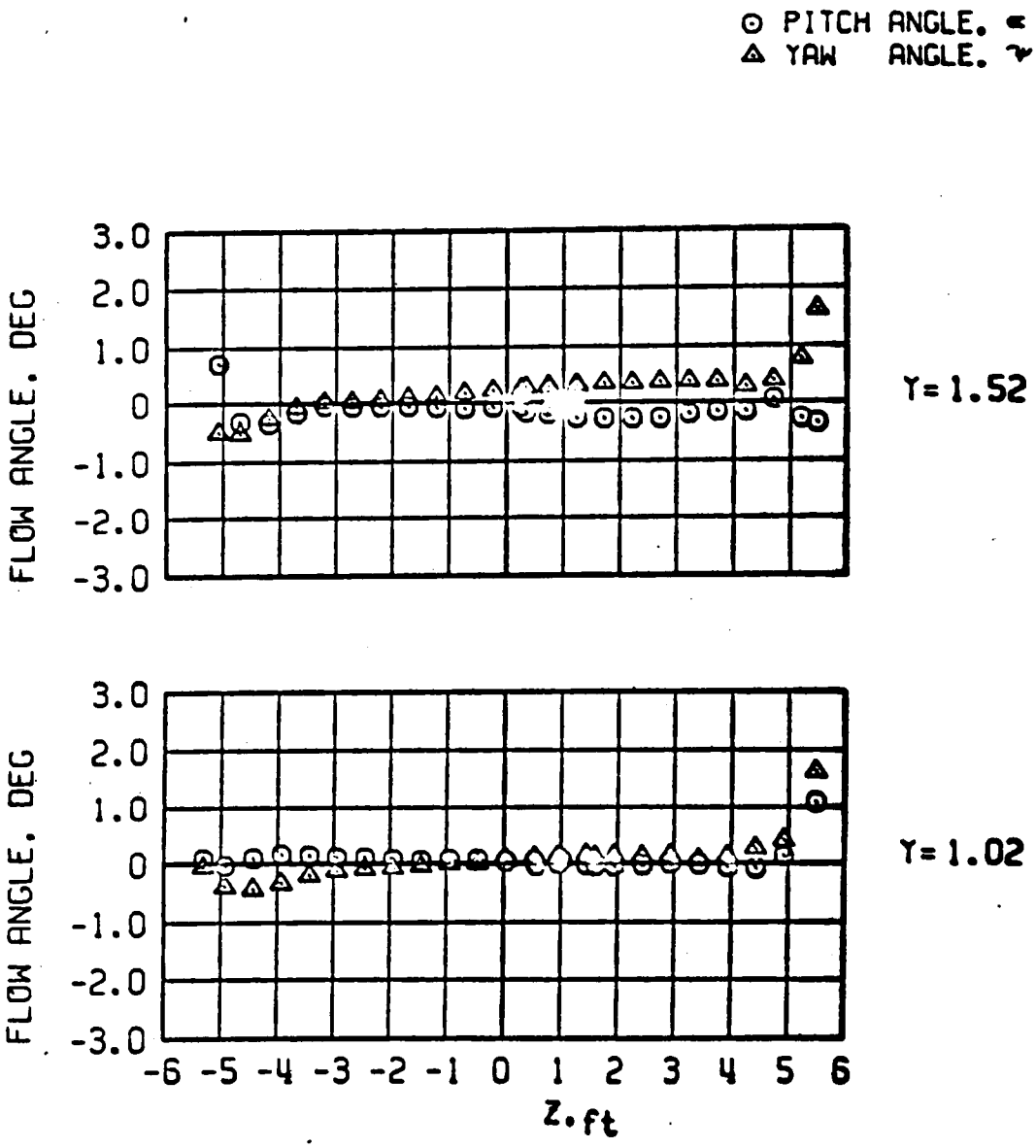

c. y = -1.0 and -0.5 inches

Figure 10. (Continued)



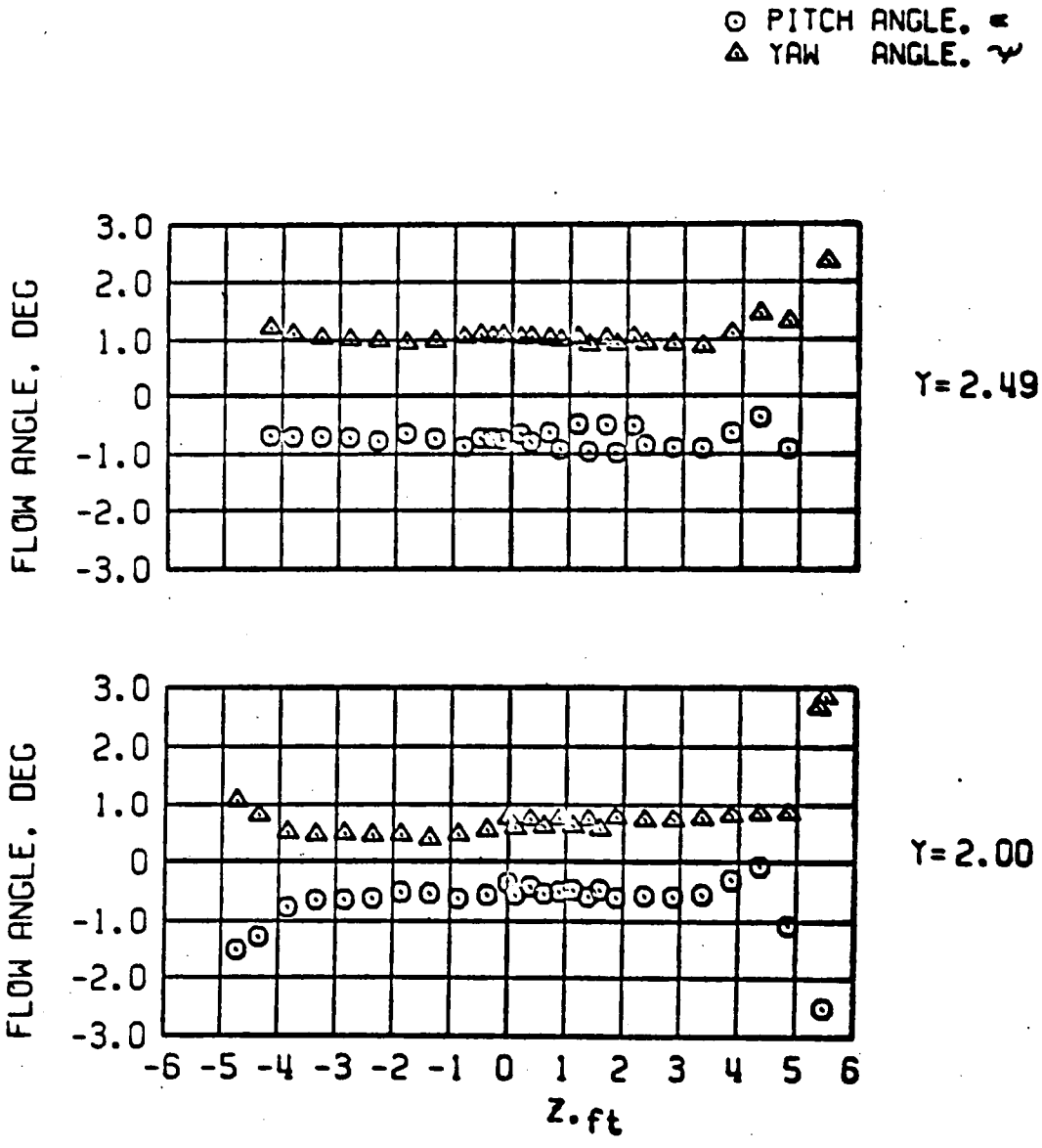

d. y = 0 and 0.5 inches

Figure 10. (Continued)



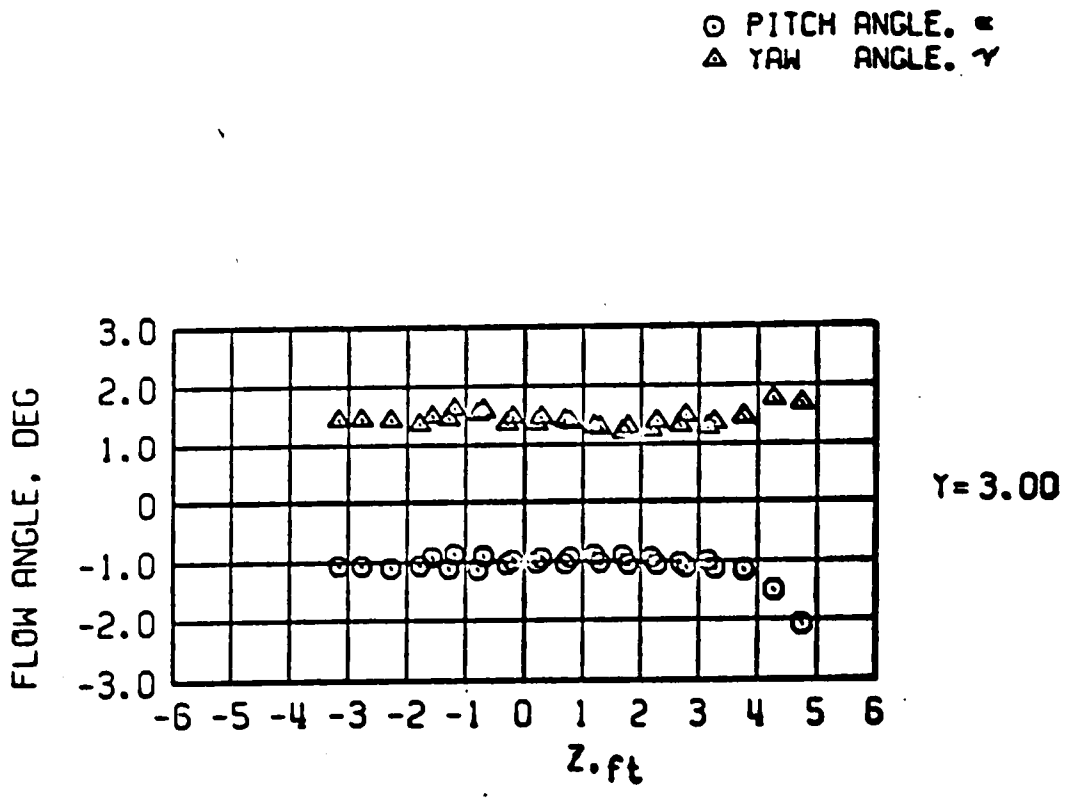

e. y = 1.0 and 1.5 inches

Figure 10. (Continued)



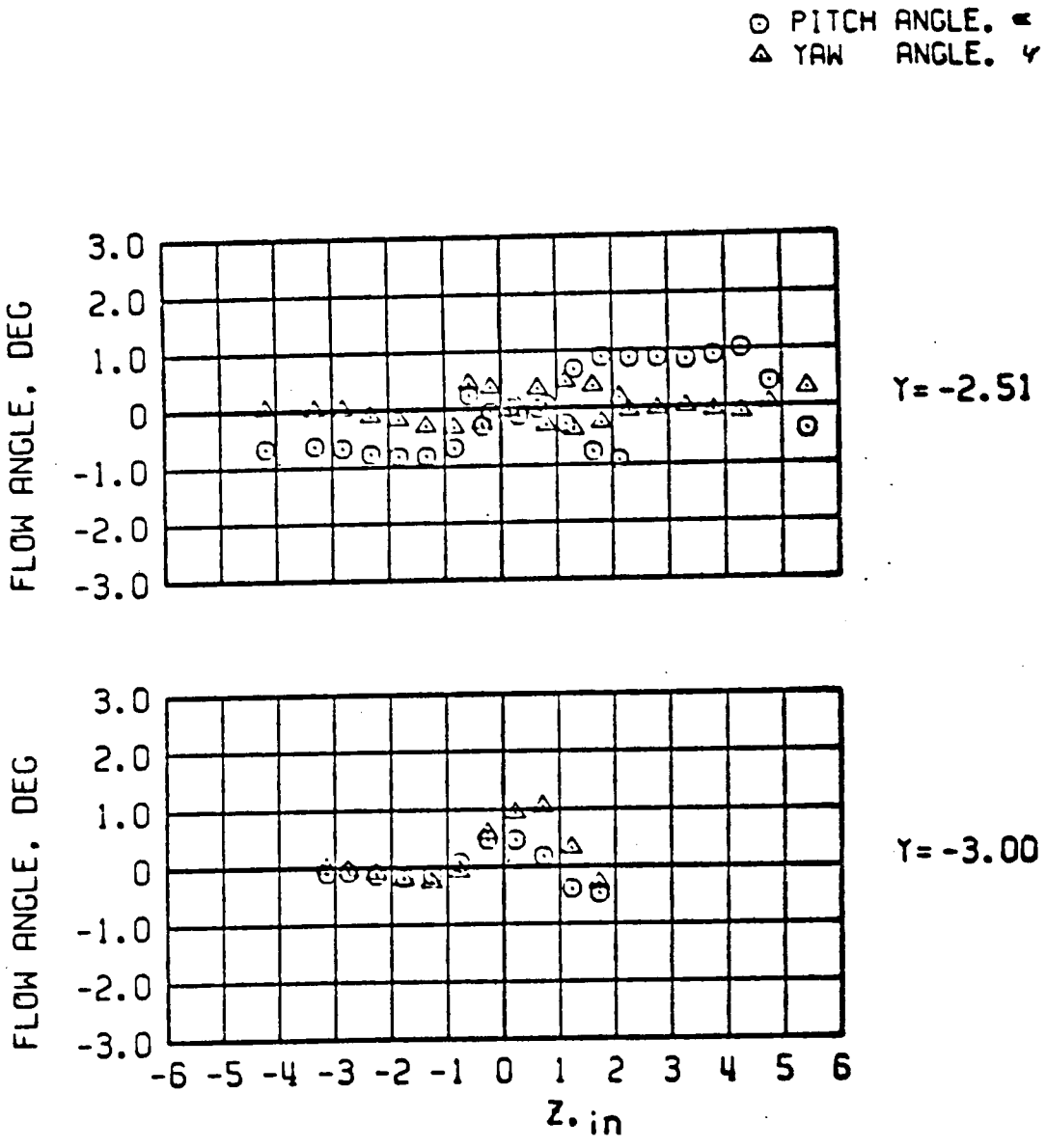

f. y = 2.0 and 2.5 inches

Figure 10. (Continued)



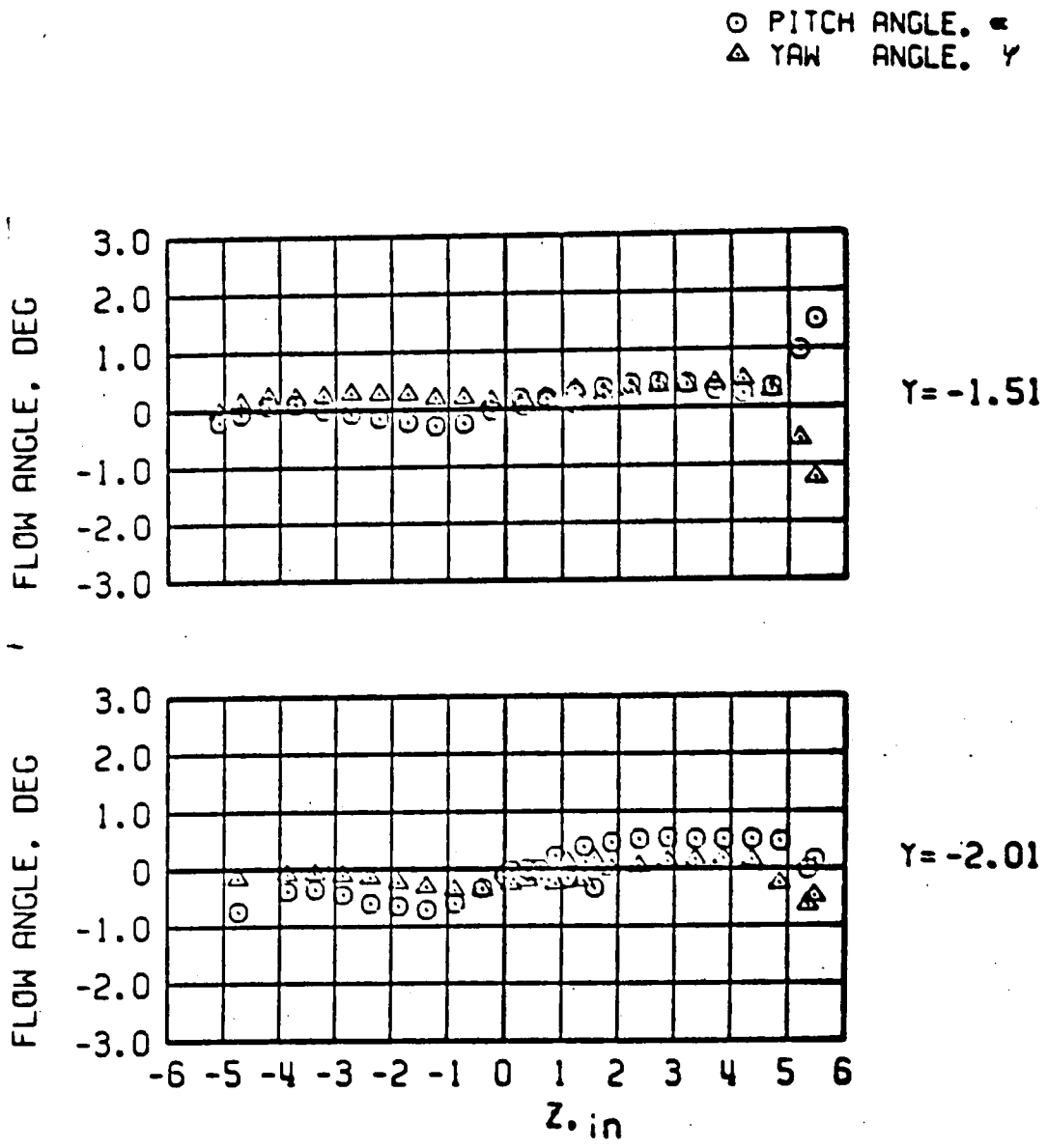

g. y = 3.0 inches

Figure 10. (Continued)



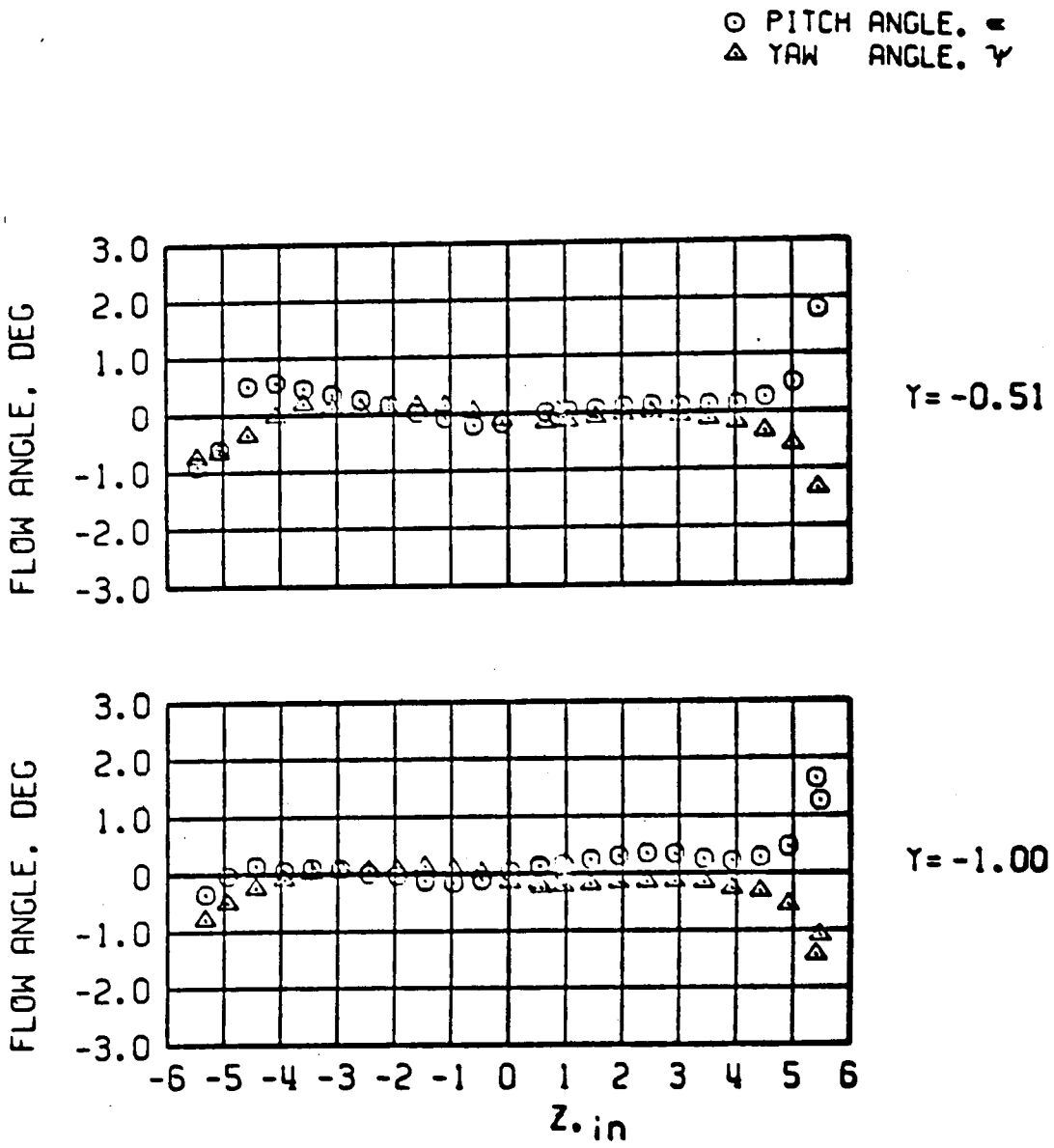

a. y = -3.0 and -2.5 inches

Figure 11. The variation of test section flow angularity with vertical position (z) at various lateral (y) positions for the open stilling chamber with the cruciform brace installed.



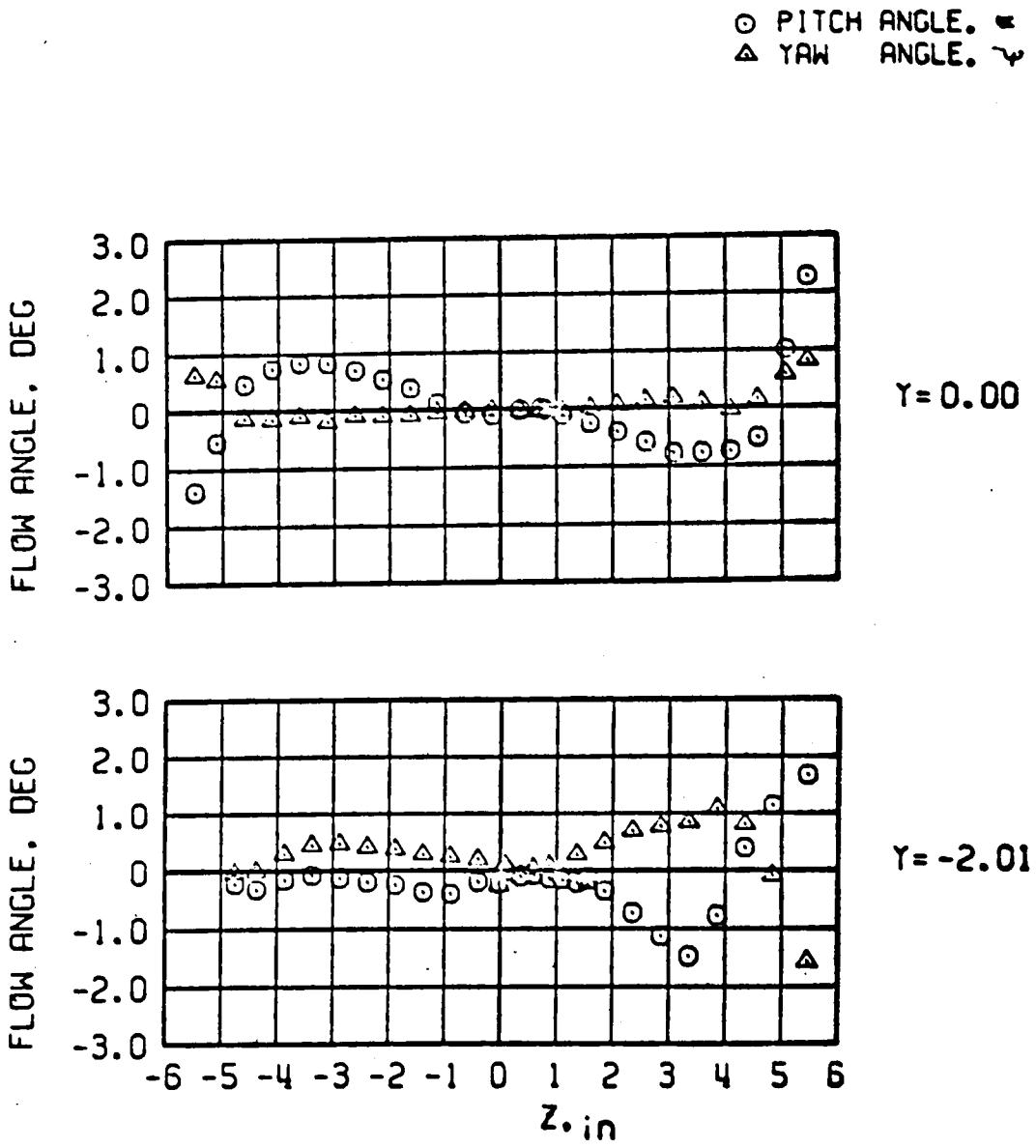

b. y = -2.0 and -1.5 inches

Figure 11. (Continued)




c. y = -1.0 and -0.5 inches

Figure 11. (Continued)




d. y = -2.0 and 0 inches

Figure 11. (Continued)

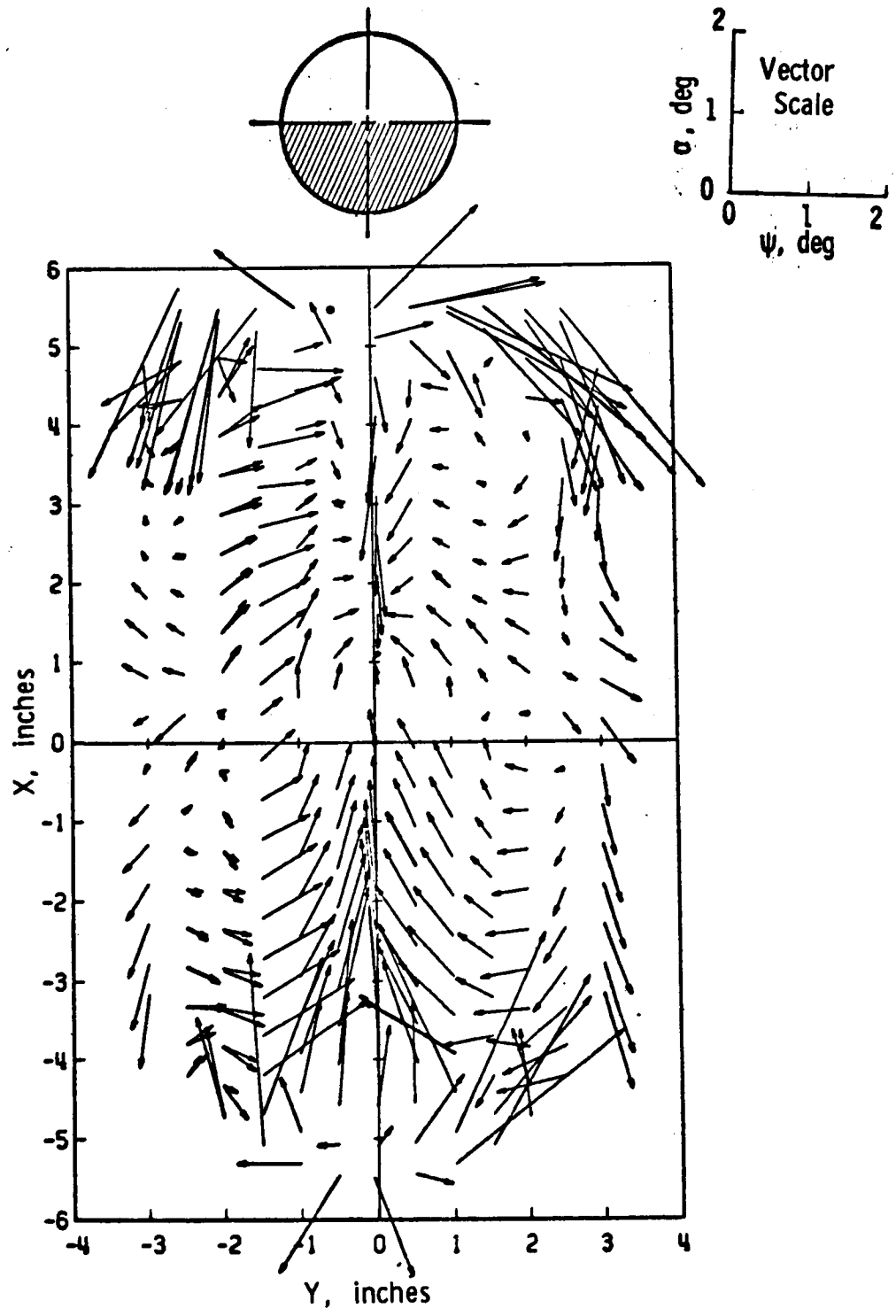



Figure 12. Resultant flow angle diagram for screen configuration 1.

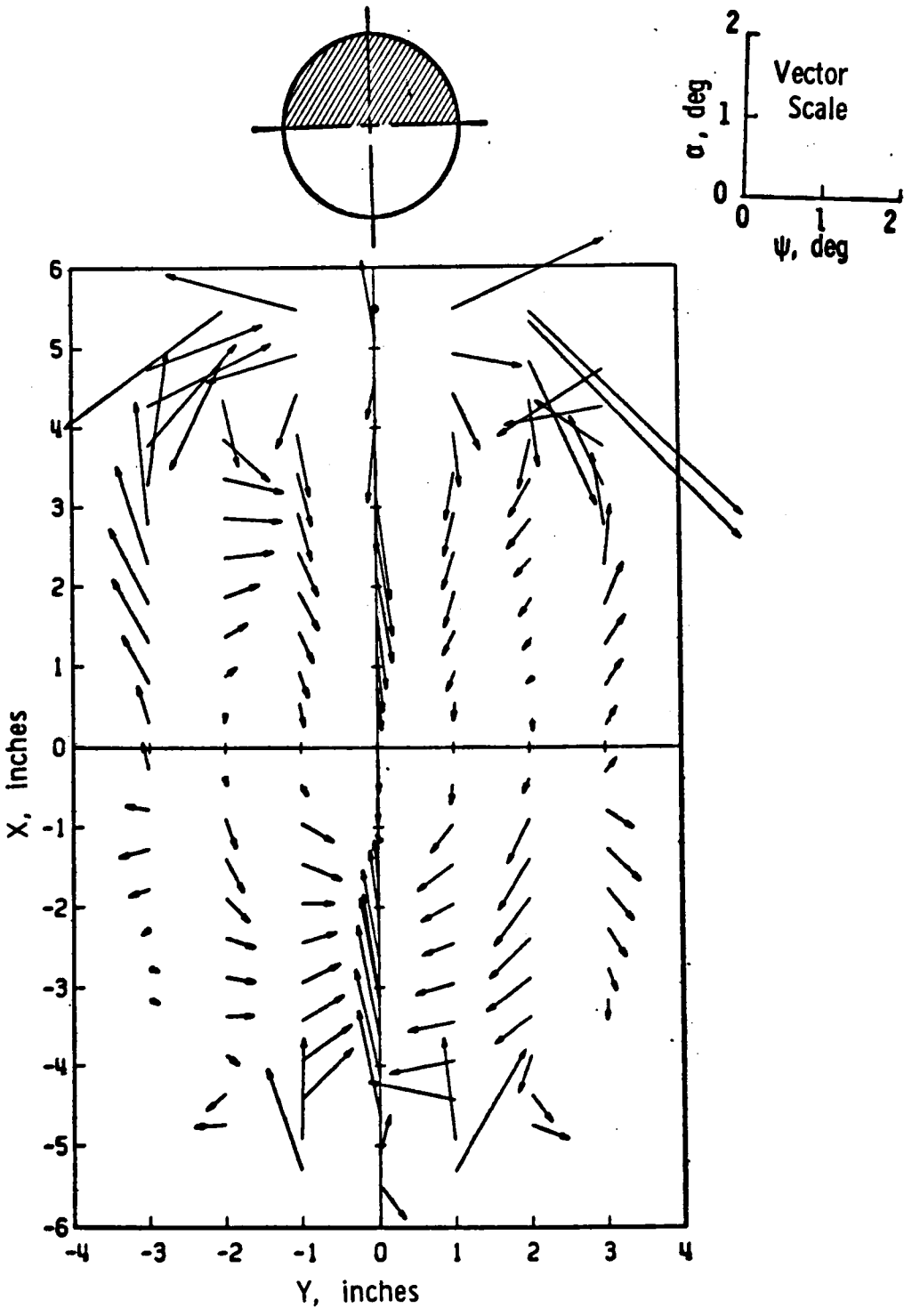



Figure 13. Resultant flow angle diagram for screen configuration 2.

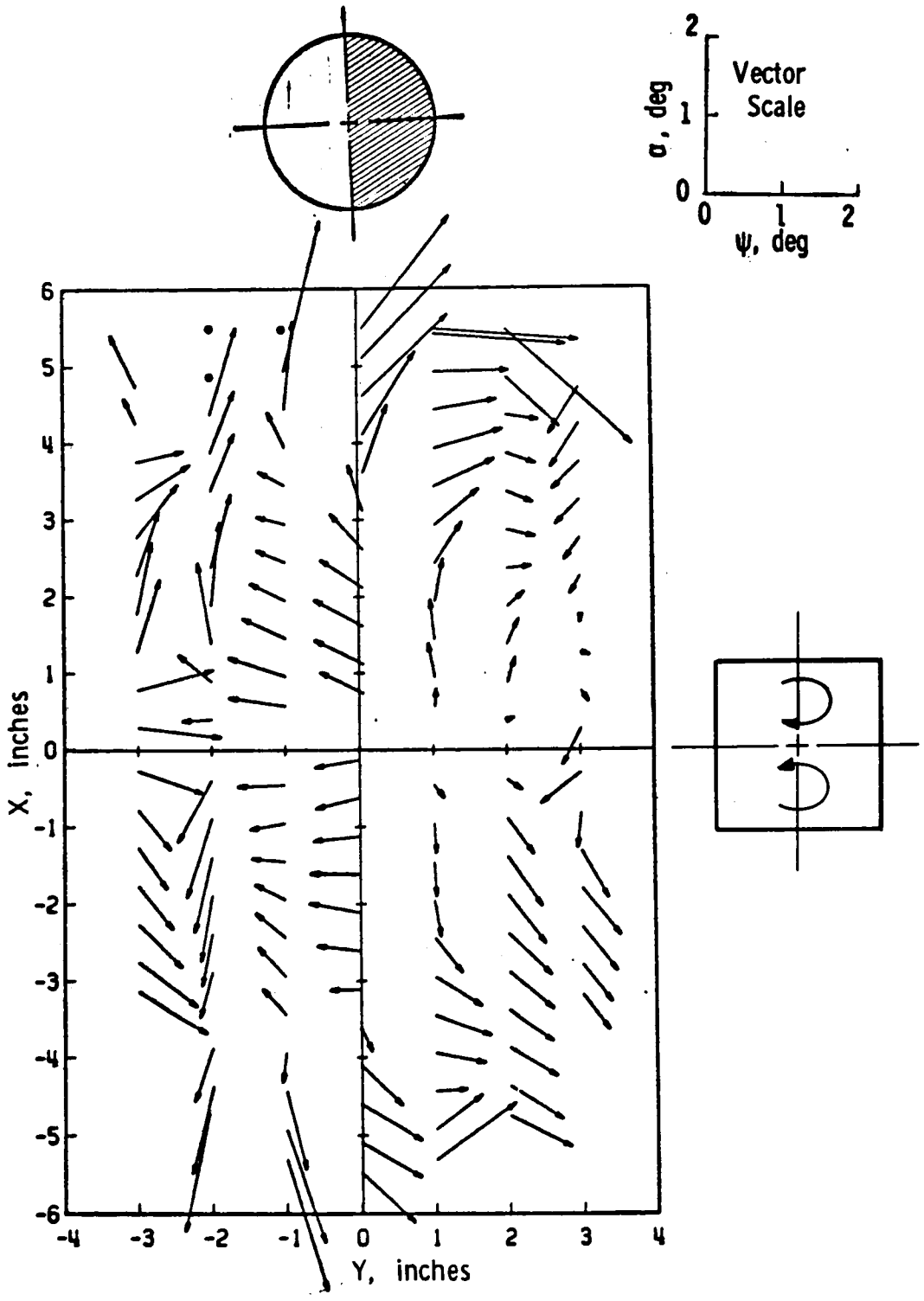



Figure 14. Resultant flow angle diagram for screen configuration 3.

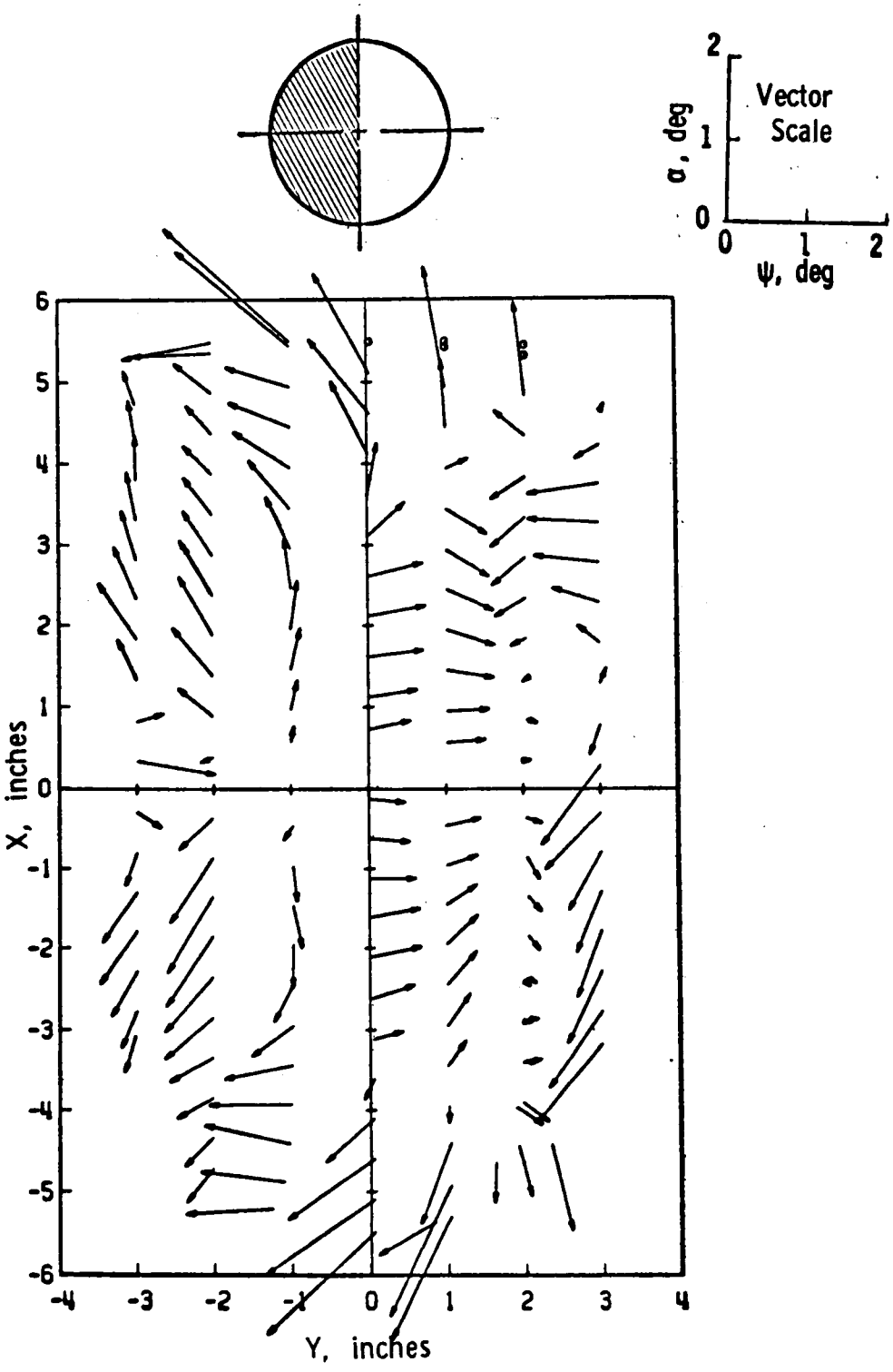



Figure 15. Resultant flow angle diagram for screen configuration 4.

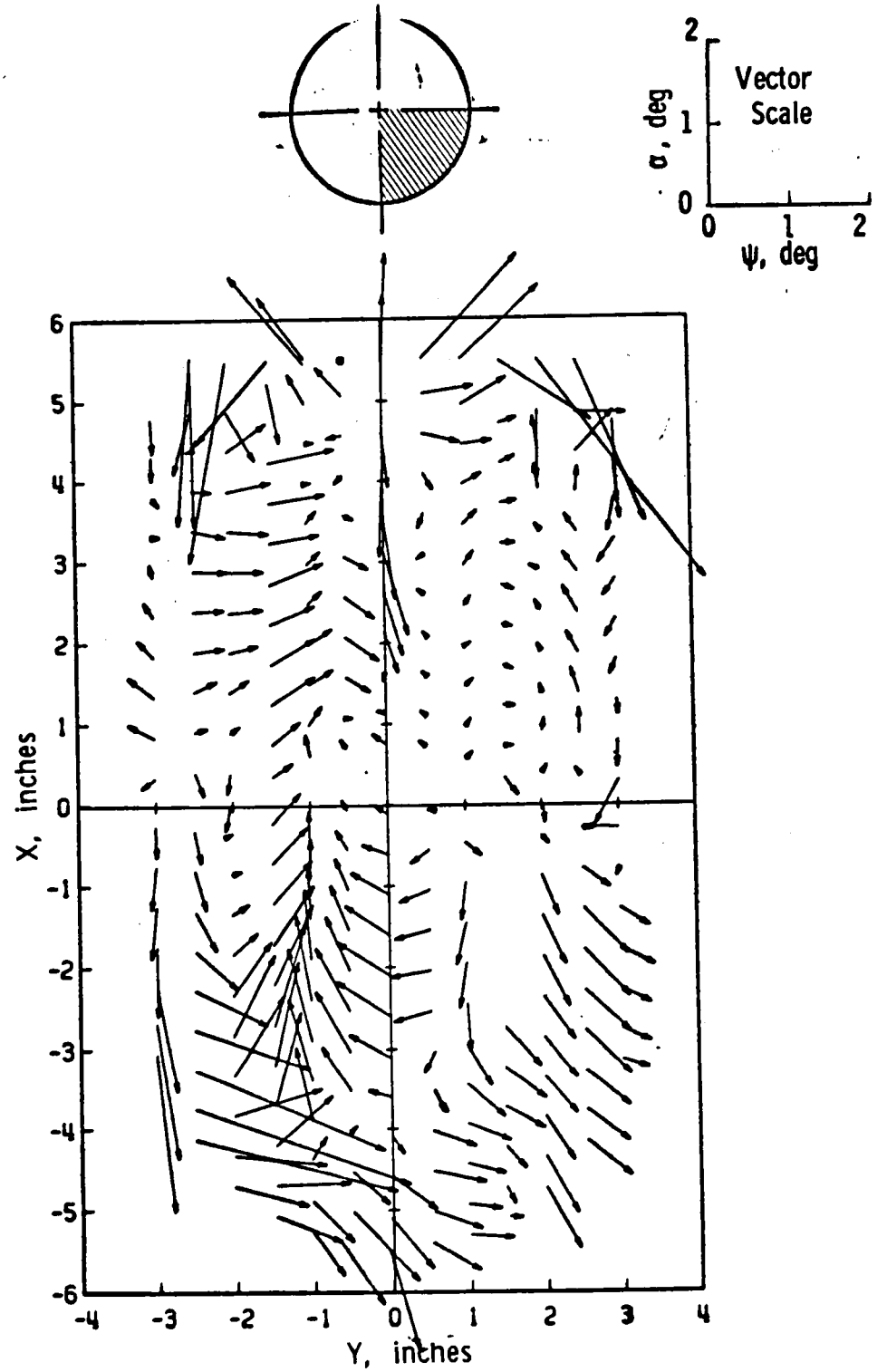



Figure 16. Resultant flow angle diagram for screen configuration 5.

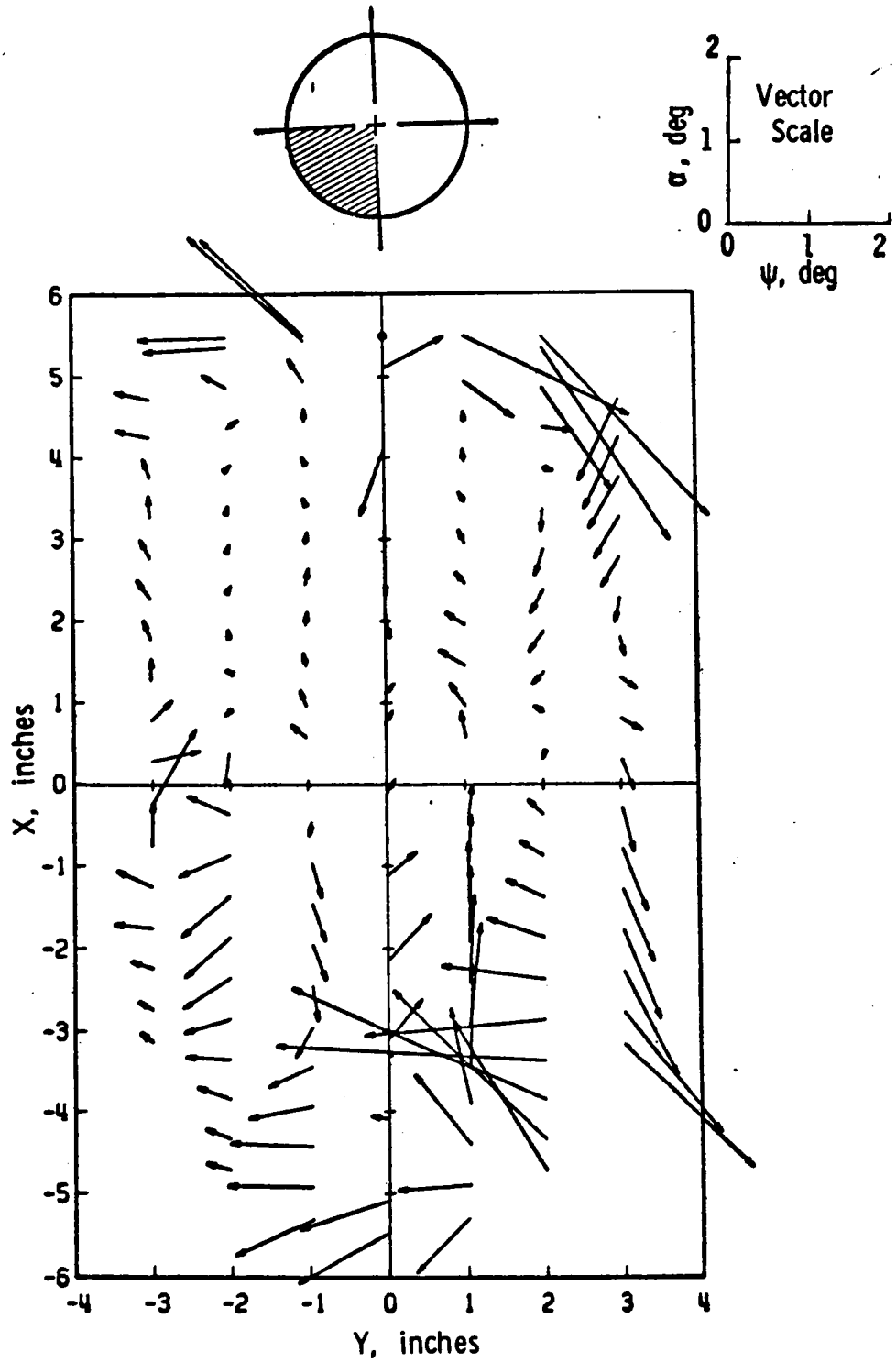



Figure 17. Resultant flow angle diagram for screen configuration 6.

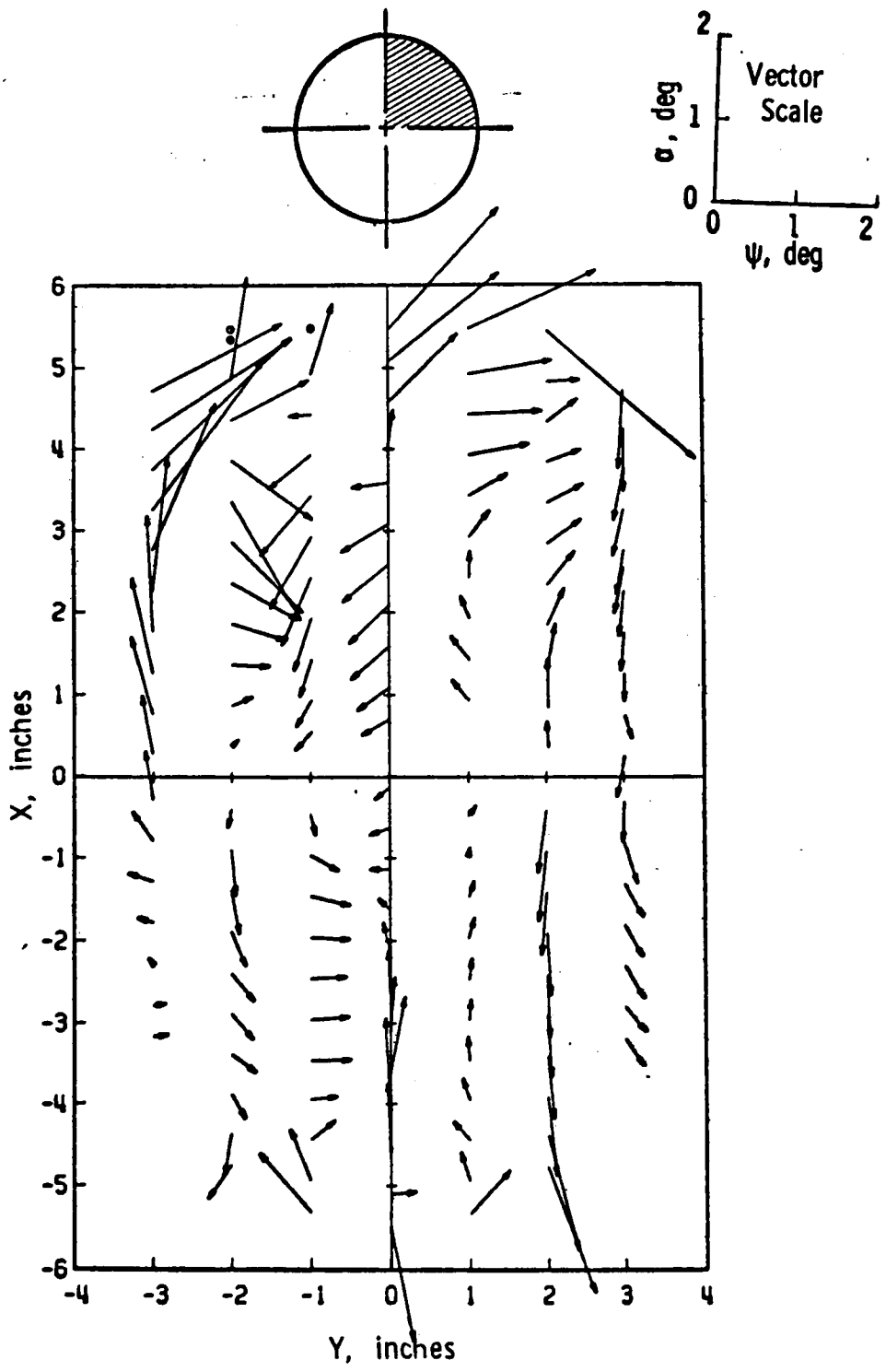



Figure 18. Resultant flow angle diagram for screen configuration 7.

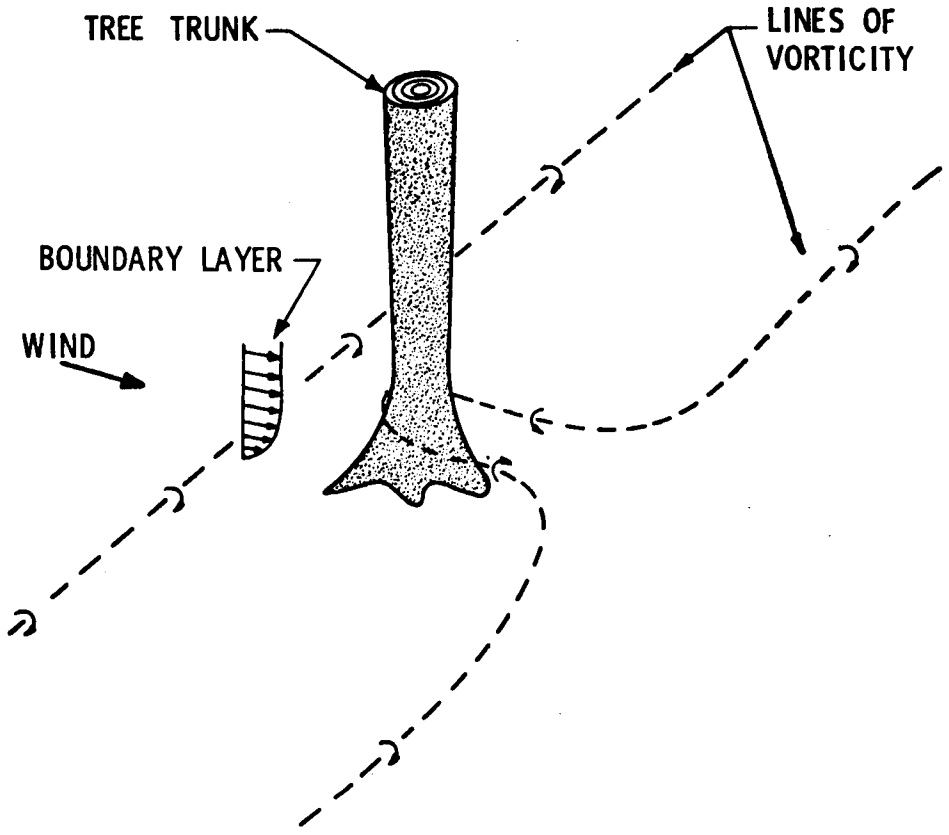



Figure 19. Distortion of lines of vorticity encountering a tree trunk.

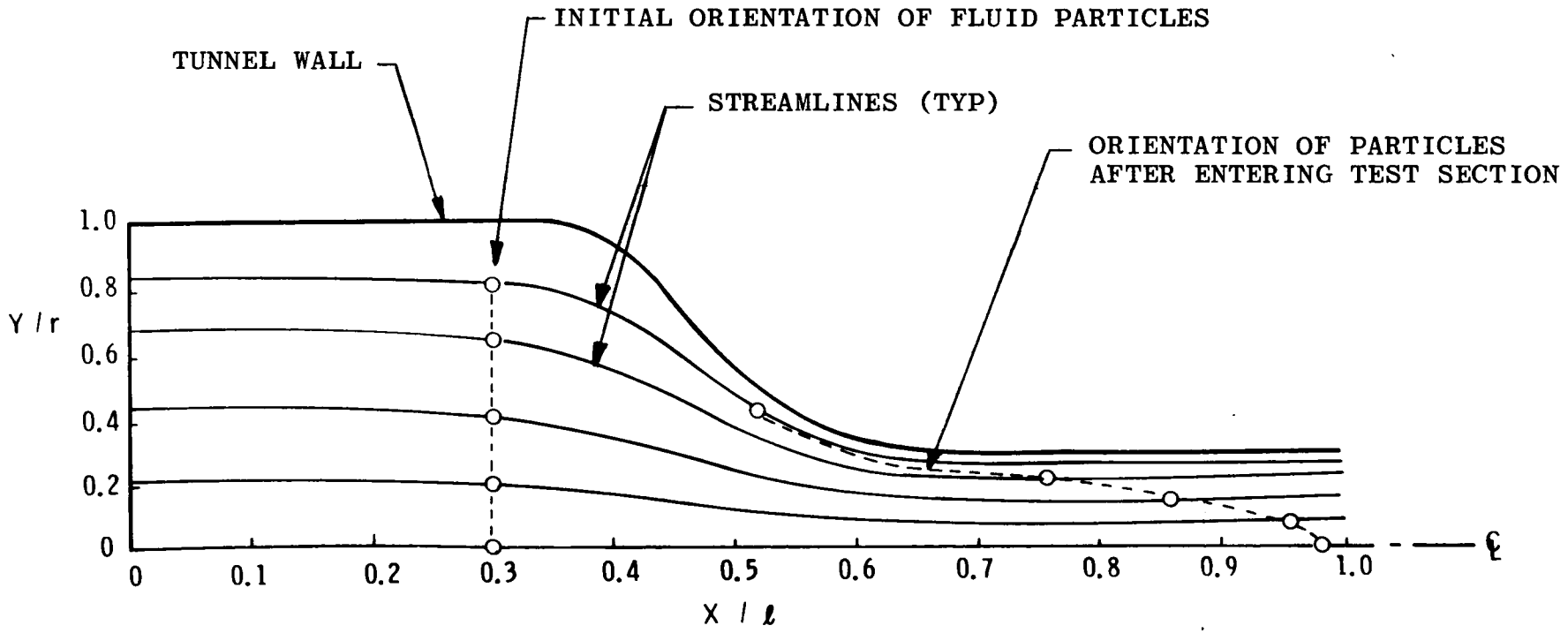



Figure 20. Streamline Pattern and Fluid Particle Displacements through a wind tunnel contraction and nozzle.

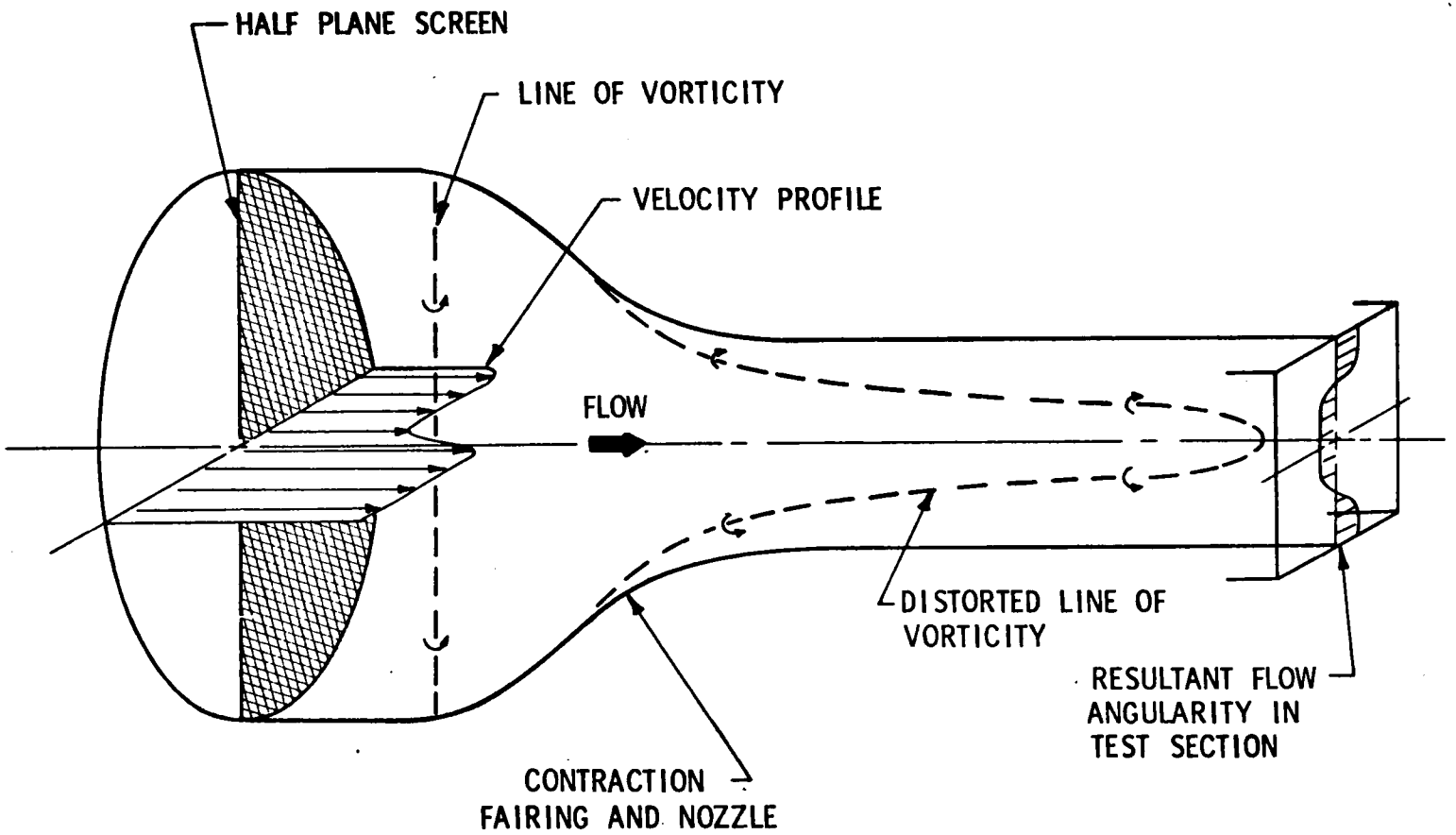
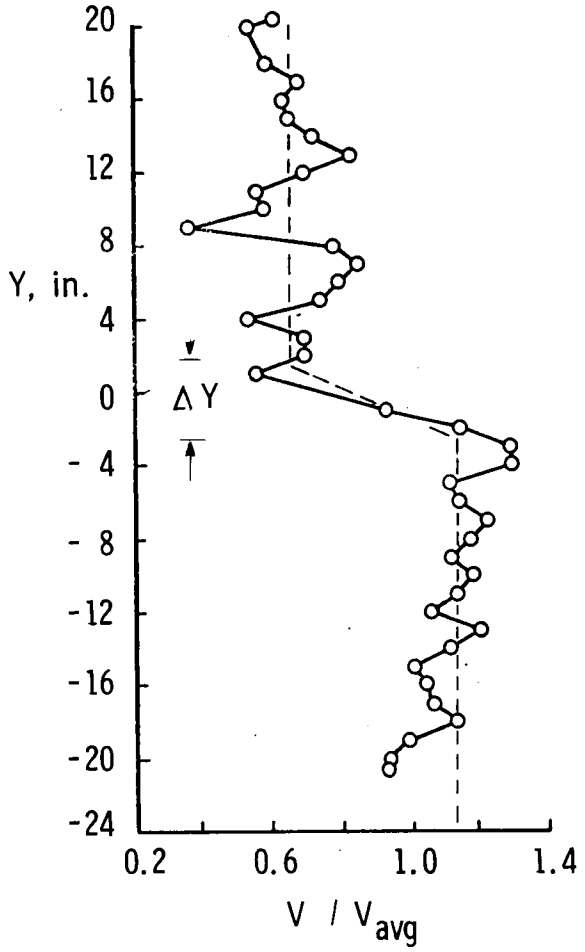
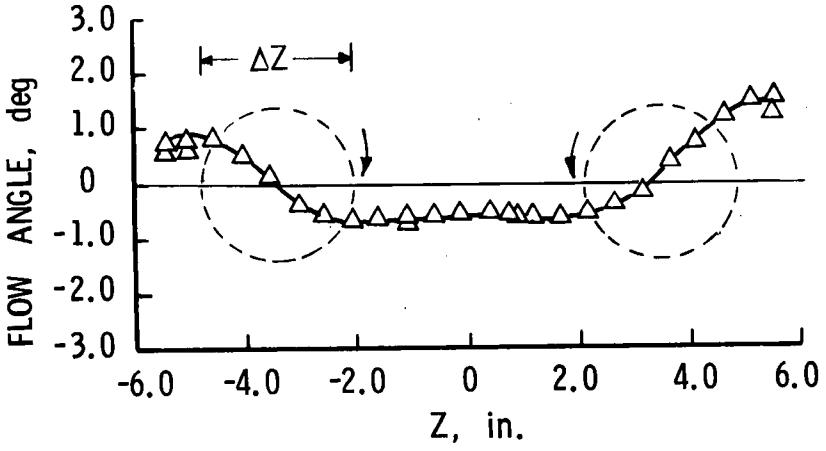



Figure 21. Illustration of the reorientation of a line of vorticity as it passes through the contraction and nozzle resulting in test section flow angularity.




a. Horizontal velocity survey in stilling chamber.




b. Test section flow angularity along vertical centerline.

Figure 22. Data obtained with the half-plane screen in the right half of the stilling chamber.

TABLE 1

STILLING CHAMBER SCREEN CONFIGURATIONS

| Configuration Number | Screen Type | Stilling Chamber* Orientation |
|---|---|---|
| 1 | Half-Plane | Lower |
| 2 | Half-Plane | Upper |
| 3 | Half-Plane | Right |
| 4 | Half-Plane | Left |
| 5 | Quarter-Plane | Lower Right |
| 6 | Quarter-Plane | Lower Left |
| 7 | Quarter-Plane | Upper Right |

*Facing upstream

# VITA

Ronald G. Lutz was born in Flint, Michigan on November 28, 1946. He graduated from high school in 1964 and enrolled in college at the Flint Junior Community College. In 1966, he enrolled at the University of Michigan, Dearborn Campus and later took part in the cooperative education program there. He became employed with ARO, Inc. at the Arnold Engineering Development Center as a cooperative student and in 1969 accepted employment there as an engineer. His Bachelor degree from Michigan is in Mechanical Engineering and since 1971 has been enrolled at the University of Tennessee Space Institute.

Since 1969 the author has been a project engineer and research engineer at both the von Kármán and Propulsion Wind Tunnel Facilities of AEDC. He has conducted various wind tunnel tests as well as technology projects related to wind tunnel performance and development. He is the author and coauthor of eight technical reports and numerous company memoranda.